1 **Interferences on Aerosol Acidity Quantification due to Gas-phase Ammonia Uptake onto**

2 **Acidic Sulfate Filter Samples**

3 Benjamin A. Nault[1,2], Pedro Campuzano-Jost[1,2], Douglas A. Day[1,2], Hongyu Guo[1,2], Duseong S.

4 Jo[1,2,*], Anne V. Handschy[1,2], Demetrios Pagonis[1,2], Jason C. Schroder[1,2,**], Melinda K.

5 Schueneman[1,2], Michael J. Cubison[3], Jack E. Dibb[4], Alma Hodzic[5], Weiwei Hu[6], Brett B. Palm[7],

6 Jose L. Jimenez[1,2]

7

8 1. Department of Chemistry, University of of Colorado, Boulder, CO, USA

9 2. Cooperative Institute for Research in Environmental Sciences, University of Colorado,

10 Boulder, CO, USA

11 3. TOFWERK AG, Boulder, CO USA

12 4. Earth Systems Research Center, Institute for the Study of Earth, Oceans, and Space,

13 University of New Hampshire, Durham, NH, USA

14 5. Atmospheric Chemistry Observations and Modeling Laboratory, National Center for

15 Atmospheric Research, Boulder, CO, USA

16 6. State Key Laboratory at Organic Geochemistry, Guangzhou, Institute of Geochemistry,

17 Chinese Academy of Sciences, Guangzhou, China

18 7. Department of Atmospheric Sciences, University of Washington, Seattle, WA, USA

19 * Now at: Advanced Study Program, National Center for Atmospheric Research, Boulder, CO

20 USA

21 ** Now at: Colorado Department of Public Health and Environment, Denver, CO, USA

22

23 Correspondence: Jose L. Jimenez (jose.jimenez@colorado.edu)

24

25

26 **Abstract**

27 Measurements of the mass concentration and chemical speciation of aerosols are important to
28 investigate their chemical and physical processing from near emission sources to the most
29 remote regions of the atmosphere. A common method to analyze aerosols is to collect them onto
30 filters and to analyze filters off-line; however, biases in some chemical components are possible
31 due to changes in the accumulated particles during the handling of the samples. Any biases
32 would impact the measured chemical composition, which in turn affects our understanding of
33 numerous physico-chemical processes and aerosol radiative properties. We show, using filters
34 collected onboard the NASA DC-8 and NSF C-130 during six different aircraft campaigns, a
35 consistent, substantial difference in ammonium mass concentration and ammonium-to-anion
36 ratios, when comparing the aerosols collected on filters versus the Aerodyne Aerosol Mass
37 Spectrometer (AMS). Another *on-line* measurement is consistent with the AMS in showing that
38 the aerosol has lower ammonium-to-anion ratios than obtained by the filters. Using a gas uptake
39 model with literature values for accommodation coefficients, we show that for ambient ammonia
40 mixing ratios greater than 10 ppbv, the time scale for ammonia reacting with acidic aerosol on
41 filter substrates is less than 30 s (typical filter handling time in the aircraft) for typical aerosol
42 volume distributions. Measurements of gas-phase ammonia inside the cabin of the DC-8 show
43 ammonia mixing ratios of 45±20 ppbv, consistent with mixing ratios observed in other indoor
44 environments. This analysis enables guidelines for filter handling to reduce ammonia uptake.
45 Finally, a more meaningful limit-of-detection for filters that either do not have an ammonia
46 scrubber and/or are handled in the presence of human emissions is ~0.2 µg m^{-3} ammonium,
47 which is substantially higher than the limit-of-detection of the ion chromatography.

Atmospheric
Measurement
Techniques
Discussions

Introduction

48

49 Particulate matter (PM), or aerosol, impacts human health, ecosystem health, visibility,

50 climate, cloud formation and lifetime, and atmospheric chemistry (Meskhidze et al., 2003;

51 Abbatt et al., 2006; Seinfeld. and Pandis, 2006; Jimenez et al., 2009; Myhre et al., 2013; Cohen

52 et al., 2017; Hodzic and Duvel, 2018; Heald and Kroll, 2020; Pye et al., 2020). Quantitative

53 measurements of the chemical composition and aerosol mass concentration are necessary to

54 understand these impacts and to constrain and improve chemical transport models (CTMs). The

55 inorganic portion of aerosol, which includes both volatile (e.g., nitrate, ammonium) and

56 non-volatile (e.g., calcium, sodium) species, controls many of these impacts through the

57 regulation of charge balance, aerosol pH, and aerosol liquid water concentration (Guo et al.,

58 2015, 2018; Hennigan et al., 2015; Nguyen et al., 2016; Pye et al., 2020). Further, the inorganic

59 portion of aerosol is an important fraction of the aerosol budget, both in polluted cities (e.g.,

60 Jimenez et al., 2009; Song et al., 2018), and remote regions (e.g., Hodzic et al., 2020), and the

61 chemistry controlling the inorganic portion of the aerosol is still not well known (e.g., Liu et al.,

62 2020).

63 There are numerous methods to quantify the inorganic aerosol composition and mass

64 concentration, including by mass spectrometry (DeCarlo et al., 2006; Canagaratna et al., 2007;

65 Pratt and Prather, 2010; Froyd et al., 2019), *on-line* ion chromatography (Talbot et al., 1997;

66 Weber et al., 2001; Nie et al., 2010), and collection onto filters to be extracted and measured

67 off-line by ion chromatography (Malm et al., 1994; Dibb et al., 2002, 2003; Coury and Dillner,

68 2009; Watson et al., 2009). Each method has different advantages and disadvantages (e.g., time

69 resolution, sample preparation, range of species identified, cost, and personnel needs). These

Atmospheric
Measurement
Techniques
Discussions
Open Access
EGU

70 results, in turn, have been used to inform and improve the results of CTMs, influencing our

71 understanding in processes such as the direct radiative effect (Wang et al., 2008b), transport of

72 ammonia in deep convection (Ge et al., 2018), aerosol pH (Pye et al., 2020; Zakoura et al., 2020)

73 and subsequent chemistry, and precursor emissions (Henze et al., 2009; Heald et al., 2012;

74 Walker et al., 2012; Mezuman et al., 2016).

75 Filter measurements have been shown to be most prone to artifacts during sample

76 collection, handling, storage of the filter, or extraction of the aerosol from the filter prior to

77 analysis. These artifacts include evaporation of volatile compounds such as organics (Watson et

78 al., 2009; Chow et al., 2010; Cheng and He, 2015) and ammonium nitrate (Hering and Cass,

79 1999; Chow et al., 2005; Nie et al., 2010; Liu et al., 2014, 2015; Heim et al., 2020), as well as

80 chemical reactions of gas-phase species with the accumulated particles (e.g., Schauer et al.,

81 2003; Dzepina et al., 2007). Further, early research indicated potential artifacts from gas-phase

82 ammonia uptake onto acidic aerosol collected onto filters, leading to a positive bias for

83 particulate ammonium (Klockow et al., 1979; Hayes et al., 1980; Koutrakis et al., 1988). This led

84 to debates about whether aerosol in the lower stratosphere was sulfuric acid or ammonium

85 sulfate (Hayes et al., 1980); however, after improved filter handling practices and *on-line*

86 measurements (i.e., mass spectrometry), it has been generally well accepted that the sulfate in the

87 stratosphere is mainly sulfuric acid (Murphy et al., 2014).

88 This artifact may impact aerosol collected in remote locations (e.g., the lower

89 stratosphere, but also the free troposphere over the Pacific Ocean basin). Comparisons for a

90 major cation, ammonium, in a similar location (middle of the Pacific Ocean) have shown very

91 different results (Dibb et al., 2003; Paulot et al., 2015). This, in turn, affects the observed charge

92 balance of cations (sulfate and nitrate) with ammonium, which can indicate different aerosol

93 phase state (Colberg et al., 2003; Wang et al., 2008a) and aerosol pH (Pye et al., 2020), leading

94 to potentially important chemical and physical differences between the real state of the particles

95 and that concluded from the measurements. An example of the differences in observed charge

96 balance of ammonium to sulfate for different studies of the same remote Pacific Ocean region is

97 highlighted in Fig. 1. This difference leads to the inorganic portion of the aerosol potentially

98 being solid (filters) and hence good ice-nucleating particles (Abbatt et al., 2006), versus it being

99 liquid (*on-line* measurements), leading to important differences in the calculated radiative

100 balance. It should be noted that other measurements (both filter and *on-line*) in a similar location

101 from another study (bar at surface (Paulot et al., 2015)) are more in-line with the *on-line*

102 observations. A large decrease in the ambient ammonia mixing ratio is required to change from

103 ammonium sulfate-like aerosols to sulfuric acid-like aerosols between the years, contradictory to

104 the increasing trends of ammonia globally (Warner et al., 2016, 2017; Weber et al., 2016; Liu et

105 al., 2019; Tao and Murphy, 2019). Further, oceanic emissions of ammonia are not high enough to

106 lead to full charge neutralization of sulfate, since these emissions are approximately an order of

107 magnitude less than those of sulfate precursors (Faloona, 2009; Paulot et al., 2015). A debate

108 about the acidity and potential impact of ammonia-uptake artifacts on acidic filters for remote

109 locations has not occurred as it did for stratospheric observations.

110   Previous laboratory studies have suggested that exposure of acidic aerosol, both

111 suspended in air in a flow tube or on a filter, to gas-phase ammonia will lead to formation of

112 ammonium salts in short time (≤ 10 s) (Klockow et al., 1979; Huntzicker et al., 1980); however,

113 it has not been investigated if this time frame applies for acidic aerosol collected on filters

Atmospheric
Measurement
Techniques
Discussions

114 handled in a typical indoor environment. Though human emissions of ammonia are variable and

115 depend on various factors (e.g., temperature, clothing, etc.) (Li et al., 2020), the emissions of

116 ammonia, specifically from perspiration but also from breath, can lead to high, accumulated

117 mixing ratios of ammonia indoor (e.g., Ampollini et al., 2019; Finewax et al., 2020) and

118 references therein), depending on the ventilation rate. The mixing ratios of ammonia can be

119 factor of 2 to 2000 higher indoor versus outdoor. This higher mixing ratio of ammonia leads to

120 similarly high mixing ratios used in prior studies to lead to partially to fully neutralize sulfuric

121 acid (Klockow et al., 1979; Huntzicker et al., 1980; Daumer et al., 1992; Liggio et al., 2011).

122   Here, we investigate whether previously observed laboratory observations of ammonium

123 uptake to acidic particulate lead to the large differences in ammonium, both in mass

124 concentration and in ammonium-to-sulfate ratios or ammonium-to-anion ratios, between *in-situ*

125 measurements and *off-line* filter measurement during five NASA and one NSF airborne

126 campaigns that sampled air over remote continental and oceanic regions. An uptake model for

127 gas-phase ammonia interacting with acidic PM on a filter along with constraints from

128 observations of gas-phase ammonia in the cabin of the airplane are used to further probe the

129 reason behind the differences between the *in-situ* and *off-line* measurements of ammonium. The

130 results provide insight into how to interpret prior aircraft measurements and other filter based

131 measurements where the filters were handled in environments (i.e., indoors), where rapid uptake

132 of ammonia to acidic PM will occur.

133

134 **2. Methods**

135 **2.1 Aircraft Campaigns**

136   Five different NASA aircraft campaigns on-board the DC-8 research aircraft and one

137 NSF aircraft campaign on-board the C-130 research aircraft are used in this study. As described

138 below, though the campaigns were sampling ambient (outside) air in various locations around the

139 world, the filters were handled and exposed to both aircraft cabin air and indoor temporary

140 laboratory air, where between 20 and 40 people were operating instruments. The campaigns

141 include the Arctic Research of the Composition of the Troposphere from Aircraft and Satellites

142 (ARCTAS) -A (April 2008) and -B (June – July 2008) campaigns (Jacob et al., 2010), the

143 Studies of Emissions and Atmospheric Composition, Clouds, and Climate Coupling by Regional

144 Surveys (SEAC^{4}RS, August – September 2013) campaign (Toon et al., 2016), the Wintertime

145 INvestigation of Transport, Emissions, and Reactivity (WINTER, February – March 2015)

146 (Schroder et al., 2018), and the Atmospheric Tomography (ATom) -1 (July – August 2016) and

147 -2 (January – February 2017) campaigns (Hodzic et al., 2020). ARCTAS-A was based in

148 Fairbanks, Alaska, Thule, Greenland, and Iqaluit, Nunavut, and sampled the Arctic Ocean and

149 Arctic regions of Alaska, Canada, and Greenland; while, ARCTAS-B was based in Cold Lake,

150 Alberta, Canada, and sampled the boreal Canadian forest, including wildfire smoke. SEAC^{4}RS

151 was based in Houston, Texas, and sampled biomass burning from western forest fires and

152 agricultural burns along the Mississippi River and the Southern United States, isoprene

153 chemistry over Southern United States and midwestern deciduous forests, and deep convection

154 associated with isolated thunderstorms, the North American Monsoon, and tropical depressions.

155 Finally, ATom-1 and -2 sampled the remote atmosphere over the Arctic, Pacific, Southern, and

156 Atlantic Oceans during the Northern (Southern) Hemispheric summer (winter) and winter

157 (summer).

Atmospheric
Measurement
Techniques
Discussions

EGU

Open Access

158   For ARCTAS-A, -B, and SEAC[4]RS, the general sampling scheme was regional, sampling

159 large regions at level flight tracks. ATom-1 and -2, being global in nature, only sampled at level

160 legs for short durations (5 – 15 min) at low (~300 m) and high (10 – 12 km) altitude, and did not

161 measure at level altitudes between the low and high altitude. Due to the sampling time of the

162 filters (see Sect. 2.2.2), the entirety of the ascent and descent time was needed for one filter

163 sample. Therefore, all data during the ascents and descents have not been considered in this

164 study to minimize any issues due to the mixing of aerosols of different compositions and

165 acidities.

166

167 **2.2 Aerosol Measurements**

168 **2.2.1 Aerosol Mass Spectrometer**

169   An Aerodyne High-Resolution Time-of-Flight Aerosol Mass Spectrometer, flown by the

170 University of Colorado-Boulder (CU for short), was flown during the five campaigns used here.

171 The general features of the AMS have been described in prior studies (DeCarlo et al., 2006;

172 Canagaratna et al., 2007), and the specifics of the CU AMS for each campaign has been

173 described elsewhere (Cubison et al., 2011; Liu et al., 2017; Nault et al., 2018; Schroder et al.,

174 2018; Guo et al., 2020; Hodzic et al., 2020). In brief, the AMS measured the mass concentration

175 of non-refractory species in PM_1 (PM with an aerodynamic diameter less than 1 μm, see Guo et

176 al. (2020) for details). Ambient air was sampled by drawing air through an NCAR

177 High-Performance Instrumental Platform for Environmental Modular Inlet (HIMIL; Stith et al.

178 (2009)) at a constant standard flow rate of 9 L min^{-1} (T = 273.15 K and P = 1013 hPa). No active

179 drying of the sampling flow was used to minimize artifacts for semi-volatile species, but the

180 temperature differential between ambient and cabin typically ensured the relative humidity (RH)

181 inside the sampling line less than 40% (e.g., Nault et al., 2018). An exception to this was during

182 ATom-1 and -2, where the cabin temperature, along with the high RH in tropics, led to higher RH

183 in the sample lines in a few instances in the boundary layer, which was accounted for in the final

184 mass concentrations (Guo et al., 2020). The air sample was introduced into the AMS via an

185 aerodynamic focusing lens (Zhang et al., 2002, 2004), which was operated at 2.00 hPa (1.50

186 Torr), via a pressure-controlled inlet, which was operated at various pressures (94-325 Torr)

187 (Bahreini et al., 2008), depending on the ceiling of the campaign and lens transmission

188 calibrations (Hu et al., 2017b; Nault et al., 2018). The aerosol, once focused, was introduced into

189 a detection chamber after three differential pumping stages. The aerosol impacted on an inverted

190 cone porous tungsten "standard" vaporizer under high vacuum, which was held at ~600°C. Upon

191 impaction, the non-refractory portion of the aerosol (organic, ammonium, nitrate, sulfate, and

192 chloride) were flash-vaporized, and the vapors were ionized by 70 eV electron ionization. The

193 ions were then extracted and analyzed with a H-TOF time-of-flight mass spectrometer (Tofwerk

194 AG). The AMS was operated in the "V-mode" ion path (DeCarlo et al., 2006), with spectral

195 resolution ($m/\Delta m$) of 2500 at m/z 44 and 2800 at m/z 184. The collection efficiency (CE) for

196 AMS was estimated with the parameterization of Middlebrook et al. (2012), which has been

197 shown to perform well for ambient aerosols (Hu et al., 2017a, 2020). The AMS nominally

198 samples aerosol with vacuum aerodynamic diameter between 40 nm and 1400 nm, which was

199 calibrated for in SEAC[4]RS, ATom-1, and -2 (Liu et al., 2017; Guo et al., 2020). Software

200 packages Squirrel and PIKA under Igor Pro 7 (WaveMetrics, Lake Oswego, OR) (DeCarlo et

201 al., 2006; Sueper, 2018) were used to analyze all AMS data.

Atmospheric
Measurement
Techniques
Discussions

202   A cryogenic pump, to reduce background of ammonium and organics (Nault et al., 2018;

203   Schroder et al., 2018), was flown on the AMS for SEAC[4]RS, ATom-1, and -2; but not for

204   ARCTAS-A and -B. The cryogenic pump lowers the temperature of a copper cylinder

205   surrounding the vaporizer to ~90 K. This freezes out the background gases and ensures low

206   detection limits from the beginning of the flight, which is critical since aircraft instruments can

207   typically not be pumped continuously and hence suffer from high backgrounds at switch-on. The

208   2σ accuracy for the AMS for inorganic aerosol is estimated to be 35% (Bahreini et al., 2009; Guo

209   et al., 2020).

210

211   **2.2.2 Aerosol Filters**

212   Fast collection of aerosol particles onto filters during airborne sampling, via the

213   University of New Hampshire Soluble Acidic Gases and Aerosol (SAGA) technique, has been

214   described elsewhere (Dibb et al., 2002, 2003), and was flown during the five campaigns

215   investigated here. Briefly, air is sampled into the airplane via a curved leading edge nozzle (Dibb

216   et al., 2002). The inlet is operated isokinetically during flight, and typically has a 50% collection

217   efficiency for aerosol with an aerodynamic diameter of 4.1 µm (Dibb et al., 2002; McNaughton

218   et al., 2007), with some altitude dependence (Guo et al., 2020). Aerosol was collected onto

219   Millipore Fluoropore Teflon filters (90 mm diameter with 1 µm pore size). Collection time was

220   dependent on altitude and estimated mass concentration, but generally 2 to 3 sm^3 (where sm^3 is

221   standard m^{-3} at temperature = 273 K and pressure = 1013 hPa) volume of air is collected to

222   ensure detectable masses of species (Dibb et al., 2002). The filters were contained in a Delrin

223   holder during collection. After collection, the filters were transferred to a particle free

224 polyethylene "clean room" bag, which was filled with zero air, sealed, and stored over dry ice.

225 The samples from the filters were then extracted during non-flight days with 20 mL ultrapure

226 water and preserved with 100 µL chloroform. The preserved samples were sent to the University

227 of New Hampshire, to be analyzed by ion chromatography. The estimated limit of detection for

228 both sulfate and ammonium is 0.01 µg sm^{-3} for all missions evaluated here (Dibb et al., 1999).

229

2.2.3 Other Aerosol Measurements

231   The NOAA Particle Analysis by Laser Mass Spectrometer (herein PALMS) was flown

232 during ATom-1 and -2. Details of the PALMS instrument configured for ATom-1 and -2 are

233 described in Froyd et al. (2019). Briefly, PALMS measures the chemical composition of single

234 aerosol particles via laser-ablation/ionization (Murphy and Thomson, 1995; Thomson et al.,

235 2000), where the ions are extracted and detected by a time of flight mass spectrometer. The

236 instrument measures particles between 100 nm and 4.8 µm (geometric diameter) (Froyd et al.,

237 2019). The measurement of PALMS used in this study is the "sulfate acidity indicator" (Froyd et

238 al., 2009). These authors reported that in the negative ion mode, there is a prominent peak at m/z

239 97, corresponding to HSO_4^-, and another peak at m/z 195, corresponding to the cluster

240 $HSO_4^-(H_2SO_4)$. The first peak was independent of acidity; whereas, the second peak was

241 dependent on acidity. Froyd et al. (2009) calibrated the PALMS ratio of

242 $HSO_4^-(H_2SO_4)/(HSO_4^- + HSO_4^-(H_2SO_4))$ to Particle-into-Liquid Sampler (PILS) measurements to

243 achieve an estimate of ammonium balance.

Atmospheric
Measurement
Techniques
Discussions

244   Besides the chemical composition, the particle number and volume distributions are used

245 here. For SEAC[4]RS, the measurements have been described elsewhere (e.g., Liu et al., 2016).

246 The laser aerosol spectrometer (from TSI), which measured aerosol from geometric diameter 100

247 nm to 6.3 μm, is used here for volume distribution. For the ATom missions, the measurements

248 have been described elsewhere (Kupc et al., 2018; Williamson et al., 2018; Brock et al., 2019).

249 Briefly, the dry particle size distribution, from geometric diameter of 2.7 nm to 4.8 μm, were

250 measured by a series of optical particle spectrometers, including the Nucleation Model Aerosol

251 Size Spectrometer (3 nm to 60 nm, custom built (Williamson et al., 2018)), an Ultra-High

252 Sensitivity Aerosol Spectrometer (60 nm to 1 μm) from Droplet Measurement Technologies

253 (Kupc et al., 2018)), and Laser Aerosol Spectrometer (120 nm to 4.8 μm) from TSI). These

254 measurements have been split in nucleation mode (3 to 12 nm), Aitken mode (12 to 60 nm),

255 accumulation mode (60 to 500 nm) and coarse mode (500 nm to 4.8 μm).

256

257 **2.3 Gas-Phase and Other Measurements**

258 **2.3.1 Ammonia Measurements**

259   Gas-phase ammonia was measured inside the cabin of the NASA DC-8 during the

260 FIREX-AQ campaign (Warneke et al., 2018), a subsequent DC-8 campaign which shared many

261 instrument installations and a similar level of aircraft personnel with the campaigns analyzed

262 here. The location of the instrument and where it sampled cabin ammonia (in relation to where

263 the SAGA filters are located) is shown in Fig. S1. Ammonia was measured by a Picarro G2103

264 Gas Concentration Analyzer (von Bobrutzki et al., 2010; Sun et al., 2015; Kamp et al., 2019).

265 The instrument is a continuous, cavity ring-down spectrometer. Cabin air is brought into a cavity

Atmospheric
Measurement
Techniques
Discussions

266 at low pressure (18.7 kPa, 140 Torr), where laser light is pulsed into the cavity. The light is

267 reflected by mirrors in the cavity, providing an effective path length of kilometers. A portion of

268 the light penetrates the mirrors, reaching the detectors, where the intensity of the light is

269 measured to determine the mixing ratio of ammonia from the time decay of the light intensity via

270 Beer-Lambert Law. The instrument measures the absorption of infrared light from 6548.5 to

271 6549.2 cm^{-1} (Martin et al., 2016). Absorption of gas-phase water is also measured and corrected

272 for. This water vapor measurement is also used to calculate RH inside the cabin of the DC-8

273 (Filges et al., 2018). Data was logged at 1 Hz.

274

275 **2.3.2 Carbon Dioxide and Temperature Measurements**

276   Carbon dioxide inside the cabin of the NASA DC-8 during FIREX-AQ was measured by

277 a HOBO MX1102 Carbon Dioxide Data Logger (HOBO by Onset). It is a self-calibrating carbon

278 dioxide sensor with a range of 0 to 5,000 ppm carbon dioxide and an accuracy of ±50 ppm. A

279 non-dispersive infrared sensor is used to measure carbon dioxide. Data was acquired once every

280 10 s to once every 2 min. Besides carbon dioxide, RH and temperature are also recorded by the

281 instrument. Prior to each flight, the instrument was turned on and measured ambient carbon

282 dioxide, outside the cabin of the DC-8, to ensure the accuracy of the instrument compared to

283 ambient carbon dioxide measurements.

284   Ambient carbon dioxide during FIREX-AQ was measured by an updated version of the

285 instrument known as Atmospheric Vertical Observations of CO_2 in the Earth's Troposphere

286 (AVOCET) (Vay et al., 2003, 2011). The updated instrument used a modified LI-COR model

287 7000 non-dispersive infrared spectrometer and measured carbon dioxide at 5 Hz.

Atmospheric
Measurement
Techniques
Discussions

288   Temperature in the cabin was measured by a thermocouple (SEAC[4]RS) or thermistor

289 (ATom-1 and 2) located in the AMS rack or a Vaisala probe located at the front of the airplane

290 (ARCTAS-A, -B, and SEAC[4]RS).

291

2.4 Theoretical Ammonia Flux Model

293   To investigate the possibility that the ammonia mixing ratio in the cabin of the DC-8 is

294 high enough to be taken up by acidic PM on a filter during the short time the filter is exposed to

295 cabin air prior to final storage, a theoretical uptake model was constructed to estimate the time

296 scale for ammonia to interact with all the acidic particles (Seinfeld. and Pandis, 2006). The

297 equations used for the model can be found in the Supplemental Information (Sect. S2). The

298 model was initialized with a range of ammonia mixing ratios (1 to 200 ppb) and a range of PM

299 diameters (10 to 1000 nm). The calculations were conducted at 298 K, which is within ±10 K of

300 typical temperatures inside the cabin of the NASA DC-8 during the five campaigns (Fig. S2). An

301 accommodation coefficient of 1 for ammonia onto acidic PM was assumed (Hanson and

302 Kosciuch, 2003), with a density of 1.8 g cm^{-3} for sulfuric acid (Rumble, 2019). For the mass

303 transfer calculations, the transition regime (between the free molecular and continuum regimes)

304 equations were used, using the Fuchs and Sutugin parameterization (Fuchs and Sutugin, 1971).

305 The model was used to estimate the ammonia molecular flux to acidic PM on the filter (Eq. S3).

306 Finally, the molecular flux was used to estimate the time it would take all the particles to be

307 partially neutralized by ammonia in the cabin (Eq. S4), though this may be a lower limit

308 (Robbins and Cadle, 1958; Daumer et al., 1992).

309

Atmospheric
Measurement
Techniques
Discussions

3. Results and Discussion

3.1 Comparison of On-Line and Off-Line Ion Balances across the Tropospheric Column

310

311

312   SAGA and AMS co-sampled aerosols during multiple aircraft campaigns. Nitrate quickly

313 evaporates from aerosols as the aerosols are transported away from source regions and is

314 typically small in the global troposphere (DeCarlo et al., 2008; Hennigan et al., 2008; Hodzic et

315 al., 2020). Thus, in Fig. 2 the mass concentrations for the two most important submicron

316 contributors to ammonium balance, ammonium and sulfate, are compared from the aircraft

317 campaigns. The campaigns generally sampled remote air, either continental or oceanic, except

318 for biomass burning sampled during ARCTAS-B and SEAC[4]RS and downwind of urban areas

319 during WINTER. The measurements, for mass concentrations greater than 0.1 μg sm^{-3}, are

320 generally within the combined uncertainties of the two instruments. Sulfate generally remains on

321 the one-to-one line, even at low mass concentrations. However, ammonium shows a large

322 divergence between the two measurements for mass concentrations less than 0.1 μg sm^{-3} during

323 all six aircraft campaigns. As shown in Fig. 2, the divergence in ammonium occurs well above

324 the limit-of-detection for both instruments, namely ~4 ng sm^{-3} for AMS for a 5-minute average

325 (DeCarlo et al., 2006; Guo et al., 2020) and 10 ng sm^{-3} for SAGA (Dibb et al., 1999), for both

326 ammonium and sulfate.

327   This divergence in ammonium mass concentration is thus reflected in the ammonium

328 balance, defined as the ratio of ammonium to sulfate plus nitrate, in moles (Fig. 3). For all

329 campaigns, the two measurements show differences in ammonium balance, especially at higher

330 altitudes, where the aerosols is distant from ammonia emissions (Dentener and Crutzen, 1994;

331 Paulot et al., 2015), but sulfate production can continue due to vertical transport of precursors

Atmospheric
Measurement
Techniques
Discussions

Open Access

EGU

332 such as SO_2. On average, the SAGA measurements indicate ammonium balance rarely below 0.5

333 throughout the troposphere; whereas, the AMS measurements indicate that ammonium balance

334 generally drops to below 0.2 for pressures less than 400 hPa. Fig. 2 and Fig. 3 indicate either

335 differences in the ammonium balance due to differences in aerosols population sampled, as

336 SAGA measures larger aerosols diameters than AMS (Guo et al., 2020), or potential artifacts

337 with one of the measurements.

338   Both the AMS and the filters sample most of the submicron aerosols (see Guo et al.

339 (2020) for details), but the filters also sample supermicron particles that the AMS does not.

340 Therefore it is possible in principle that the difference could be due to ammonium present in

341 supermicron particles. As discussed in Guo et al. (2020), nearly 100% of the measured volume

342 occurs for aerosols < 1 μm above the marine boundary layer, where the largest difference in

343 ammonium balance between the filters and AMS occurs (Fig. 3). Further, ammonium has been

344 observed to be a small fraction of the supermicron mass (Kline et al., 2004; Cozic et al., 2008;

345 Pratt and Prather, 2010), except for instances of continental fog (Yao and Zhang, 2012) and

346 Asian dust events (Heim et al., 2020). An upper estimate of supermicron ammonium can be

347 calculated using results from prior studies (Kline et al., 2004; Cozic et al., 2008). In these prior

348 studies, ~90% of the ammonium was submicron. With the average ammonium observed during

349 ATom-1 and -2 (~10 to 50 ng sm^{-3}) (Hodzic et al., 2020), that would suggest an upper limit of ~1

350 to 5 ng sm^{-3} ammonium in the supermicron aerosols. This upper estimate does not explain the

351 differences between AMS and filters during ATom-1 and -2 (Fig. S3), as the percent difference

352 increases with decreasing estimated supermicron ammonium volume. As the largest differences

353 between the AMS and filters occur well above the boundary layer (Fig. 3), away from

354 continental ammonia sources (Dentener and Crutzen, 1994) and Asian dust events, we conclude

355 that the sampling of supermicron aerosols by filters is not leading to the observed differences in

356 ammonium.

357   Prior studies by PALMS have shown aerosols observed for pressure < 400 hPa to be

358 acidic, depending on potential recent influence of boundary layer air via convection (Froyd et al.,

359 2009; Liao et al., 2015), similar to observations by other single particle mass spectrometers (Pratt

360 and Prather, 2010). Though not reaching similarly low $NH_4/(2\times SO_4)$ values as the AMS, the

361 PALMS acidity marker shows much lower values than were determined by the aerosols collected

362 on the filters (Fig. S4). Different reasons for PALMS not achieving as low values as AMS may

363 include differences in aerosols sizes sampled by PALMS versus AMS (Guo et al., 2020), and the

364 sensitivity of the acidity marker to laser power (Liao et al., 2015). Thus, two different *on-line*

365 measurements indicate that the ammonium balance is lower than the aerosols collected on filters,

366 suggesting potentially more acidic aerosols.

367   Differences in ammonium balance between AMS and SAGA are detectable for sulfate

368 mass concentrations ≤ 1 µg sm^{-3} (Fig. 4) for all six aircraft campaigns. As the sulfate mass

369 concentration decreases, the relative differences in ammonium, and thus ammonium balance,

370 increase. The large majority of the troposphere contains sulfate mass concentrations in which the

371 differences in ammonium are observed, highlighting the importance of this problem (Fig. 4a).

372 Thus, except for more polluted conditions (> 1 µg sm^{-3} sulfate), which mainly occurs in

373 continental (Jimenez et al., 2009; Kim et al., 2015; Malm et al., 2017) and urban regions

374 (Jimenez et al., 2009; Hu et al., 2016; Kim et al., 2018; Nault et al., 2018), this bias between

375 filters and *on-line* measurements is critically important, especially since airborne measurements

Atmospheric
Measurement
Techniques
Discussions

376 are often the only meaningful observational constraints for remote regions. Thus, this analysis

377 suggest that for filters handled in indoor environments with large ammonia mixing ratios (see

378 below), a more meaningful ammonium limit-of-detection would be equivalent to 1 μg sm^{-3}

379 sulfate, which would be ~0.2 μg sm^{-3} ammonium.

380

381 **3.2 Ammonia Levels on the NASA DC-8 Cabins**

382   Prior studies have suggested that various sources of ammonia could impact acidic filter

383 measurements (Klockow et al., 1979; Hayes et al., 1980; Koutrakis et al., 1988). Some of these

384 studies found that the materials of the containers where the filters are stored, unless thoroughly

385 cleaned and not stored around humans, are a source of ammonia gas that reacts with the sulfuric

386 acid on the filters to become ammonium, leading to ammonium bisulfate or ammonium sulfate

387 (Hayes et al., 1980). Further, handling of acidic filters in rooms with people or acidic aerosol in

388 the presence of human breath can also lead to near to complete neutralization of acidic aerosol

389 (Larson et al., 1977; Hayes et al., 1980; Clark et al., 1995). Finally, various studies have

390 suggested that the SAGA filters specifically may be impacted by various ammonia sources prior

391 to sampling with the ion chromatography (Dibb et al., 1999, 2000; Fisher et al., 2011).

392   During SAGA sampling, the filters with collected aerosol are moved from the sample

393 collector to a Teflon bag that is filled with clean air. During this step, the filter is exposed to the

394 cabin air of the DC-8 for ~10 s. As humans are a source of ammonia (Larson et al., 1977; Clark

395 et al., 1995; Sutton et al., 2000; Finewax et al., 2020; Li et al., 2020), this source sustains

396 significant ammonia concentrations in indoor environments, which could potentially bias the

397 filter measurements. *On-line* measurements would not be subject to this effect since the sampled

398 air is not exposed to cabin air before measurement. While inlet lines for *on-line* instruments

399 could in theory lead to some memory effects, there is no evidence of such effects in the data

400 (e.g., the response going from a large, neutralized plume into the acidic FT is nearly

401 instantaneous (Schroder et al., 2018)).

402   During a recent 2019 NASA DC-8 aircraft campaign, FIREX-AQ, ammonia was

403 measured on-board the DC-8 during several research flights. An example time series of cabin

404 ammonia, temperature, and RH is shown in Fig. 5. Prior to take-off, as scientists were slowly

405 boarding the airplane, the ammonia mixing ratio was low (< 20 ppbv) and similar to ambient

406 levels of ammonia outside the aircraft. As scientists started boarding before take-off, the

407 ammonia mixing ratio increased. Upon doors closing, the mixing ratio leveled off at ~40 ppbv.

408 After take-off, the mixing ratio remained ~40 ppbv, though there were changes related to

409 changes in cabin temperature and humidity, which would affect emission rates and also

410 adsorption of ammonia onto cabin surfaces (Sutton et al., 2000; Finewax et al., 2020; Li et al.,

411 2020) and movement of scientists throughout the cabin, which would affect emission rates and

412 their location.

413   The average (±1σ spread of the observations) and median ammonia in the cabin of the

414 DC-8 during FIREX-AQ was 45.4±19.9 and 41.9 ppbv (Fig. 6). There was a large positive tail in

415 ammonia mixing ratio, related to high temperatures (Fig. S5), which causes the scientists to

416 perspire more and release more ammonia (Sutton et al., 2000; Finewax et al., 2020; Li et al.,

417 2020). Compared to outdoor ammonia mixing ratios, ranging from urban to remote locations, the

418 ammonia in the cabin of the DC-8 is higher by a factor of 2 to 2000 (Fig. 6). On the other hand,

419 the ammonia measured in the cabin of the DC-8 is similar but towards the lower end of the

420 mixing ratios measured during various indoor studies (Table S1 for compilation of references).

421   The ammonia mixing ratios observed in the cabin were verified by investigating the cabin

422 air exchange rates (see SI Sect. S3). Using carbon dioxide measurements, the exchange rate in

423 the cabin was calculated to be 9.9 hr^{-1} (Fig. S6), which is similar to literature values for the cabin

424 exchange rate of other passenger airliners (Hunt and Space, 1994; Hocking, 1998; Brundrett,

425 2001; National Research Council, 2002). This value is a factor of 2 to 5 higher than typical

426 exchange rates for commercial buildings (Hunt and Space, 1994; Pagonis et al., 2019), which

427 would suggest lower mixing ratios than observed in other indoor environments. Using this

428 exchange rate, and the literature total ammonia emission rates from humans (1940 μg hr^{-1}

429 person^{-1} (Sutton et al., 2000)) and the average of ambient ammonia mixing ratios as an outdoor

430 background onto which the human emissions in the cabin are added (~4.4 ppbv, Fig. 6), the

431 ammonia mixing ratio in the cabin of the DC-8 was estimated to be 43.4 ppbv, which is within

432 the uncertainty of the average ammonia (45.4±19.9 ppbv) inside the cabin of the DC-8. Thus, the

433 observed ammonia mixing ratios in the cabin of the DC-8 are consistent with the cabin air

434 exchange rates and literature human ammonia emissions. These mixing ratios are approximately

435 a factor of nine higher than in a typical laboratory environment (Fig. S7), as there are fewer

436 people (1 to 4 versus 20 to 40), making the cabin of the DC-8 an extreme laboratory environment

437 for handling acidic filters. As shown in Fig. 6, ammonia mixing ratios in indoor environments

438 are high enough to change the thermodynamics of inorganic aerosol, leading to higher

439 ammonium balances (Weber et al., 2016). Thus, similar to the conclusions of other studies, the

440 cabin of the DC-8 is an important source of ammonia that could lead to biases with acidic

441 aerosols collected on filters.

442

3.3 Can Uptake of Cabin Ammonia Explain the Higher Ammonium Concentrations on

444 **Filters?**

445   As shown in Fig. 6, the cabin of the DC-8 is an important source of ammonia from the

446 breathing and perspiring of scientists. Prior studies (Klockow et al., 1979; Huntzicker et al.,

447 1980; Daumer et al., 1992; Liggio et al., 2011) have shown in laboratory settings that 10 s is fast

448 enough to partially to fully neutralize sulfuric acid. Thus, here we investigate whether the time of

449 the filter handling of 10 s will lead to partial to full neutralization of sulfuric acid from cabin

450 ammonia, or whether this time is fast enough to limit exposure of the acidic filter to cabin

451 ammonia. Huntzicker et al. (1980) showed that for typical aerosol modal distributions (Fig. 7)

452 and cabin RH (Fig. S9), an initial pure sulfuric acid aerosol, suspended in a flow reactor, reaches

453 equal molar amounts of ammonium and sulfate (i.e., ammonium bisulfate) when exposed to 70

454 ppb ammonia in 10 s. This indicates the plausibility that acidic aerosol filters, which typically

455 have lower sulfate mass concentrations than Huntzicker et al. (1980) (~2 µg versus ~55 µg

456 sulfate equivalent on filters), would interact with cabin ammonia to form at least ammonium

457 bisulfate. Further, other studies found that in less than 10 s, sulfuric acid aerosol, suspended in a

458 flow reactor, at RH ≤ 45%, will completely react with gas-phase ammonia to form ammonium

459 sulfate (Robbins and Cadle, 1958; Daumer et al., 1992). The latter study used ammonia mixing

460 ratios similar to the amount observed in the cabin of the DC-8 (~30 ppbv); whereas, the former

461 study used excess ammonia (~9 ppmv).

Atmospheric
Measurement
Techniques
Discussions

Open Access

EGU

462   First, the time of diffusion of ammonia gas from the surface to the interior of the filter

463   was investigated, as there is a potential for the PM to be embedded deep into the filter. Eq. 1

464   (Seinfeld. and Pandis, 2006):

465    $$\tau_{diffusion} = \frac{d_t^2}{8D_g}$$ Eq. 1

466   where d_t^2 is the depth of the Teflon (~0.015 cm) and D_g is the diffusion coefficient of ammonia in

467   air (0.228 cm^2 s^{-1}) (Spiller, 1989). Therefore, the estimated timescale for ammonia to diffuse

468   through the depth of the Teflon filter is ~1×10^{-4} s, meaning that the surface of PM will always be

469   in contact with cabin-level mixing ratios of ammonia.

470   A theoretical uptake model for ammonia to acidic PM on filters was run for a range of

471   ammonia mixing ratios and PM diameters (Fig. 7). As shown in Fig. 7, only at the lowest

472   ammonia mixing ratios (< 10 ppbv), the flux of ammonia to acidic PM is slower (> 20 s) than the

473   typical filter handling time (~10 s) for typical aerosol diameters in the remote atmosphere. For

474   the conditions of the DC-8, similar to other indoor environments (> 20 ppbv ammonia, Fig. 6),

475   and ambient aerosol diameters in the accumulation mode that contains most ambient sulfate (Fig.

476   7), the amount of time needed for cabin ammonia to interact with acidic PM on filters to form

477   ammonium bisulfate is ≤ 10 s, similar to the results of Huntzicker et al. (1980). Also, studies

478   show that the kinetic limitation to form ammonium sulfate ((NH_4)$_2SO_4$) versus ammonium

479   bisulfate (NH_4HSO_4) is relatively low and can occur within the 10 s time frame (Robbins and

480   Cadle, 1958; Daumer et al., 1992). A laboratory setting with ~5 ppbv NH_3 would result in the

481   filters needing to be exposed to laboratory air for at least 40 s to form ammonium bisulfate (Fig.

482   S8) versus the 3 to 10 s for conditions in the cabin of the DC-8 (Fig. 7), further exemplifying the

483   challenging conditions of the DC-8 cabin for filter sampling.

484   The prior analysis made the assumption that the PM maintained a spherical shape upon

485 impacting the Teflon filter. More viscous (i.e., solid) PM is more likely to maintain a spherical

486 shape on filters whereas less viscous (i.e., liquid) PM will spread and become more similar to

487 cylindrical shape (e.g., Slade et al., 2019). As more acidic aerosol is more likely to be liquid

488 (e.g., Murray and Bertram, 2008), an exploration of cylindrical shape was conducted. Depending

489 on the assumed height of the cylindrical shape, the timescale for a molecule of ammonia to

490 interact with a molecule of sulfuric acid decreases from ~5 s (for maximum ammonia and

491 aerosol volume) to ~4 s (assuming height of cylinder equals radius of sphere) to less than 1 s as

492 height decreases from 25 nm or less. The aerosol deforming and spreading upon impacting the

493 filters increases the particle surface area, and decreases the amount of time for cabin ammonium

494 to interact with the acidic PM. Thus, less viscous aerosol has more rapid uptake and interaction

495 with ammonia due to the higher surface area.

496   A potential limitation to the model is the accommodation coefficient of ammonia to

497 acidic PM, as there are conflicting reports on its value (Hanson and Kosciuch, 2004; Worsnop et

498 al., 2004). However, as shown in Worsnop et al. (2004), once the sulfuric acid weight percentage

499 is 50% or greater, the different studies converge to an accommodation coefficient of ~1. Various

500 studies indicate that the RH in the cabin of jet airplanes is low due to how air is brought into the

501 airplane, typically < 20% (Hunt and Space, 1994; Brundrett, 2001; National Research Council,

502 2002). Even though the ambient RH may be higher than the RH in the cabin of the DC-8, the

503 water equilibration is rapid (< 1 s) for the temperature of the cabin of the DC-8, even for very

504 viscous aerosol (Shiraiwa et al., 2011; Price et al., 2015; Ma et al., 2019), meaning the PM on the

505 filter would rapidly reach equilibrium with the cabin RH upon exposure. This would result in a ≥

506 60% sulfuric acid weight percentage (Wilson, 1921) for the typical RH ranges in the cabin of

507 typical airlines. However, various measurements in the DC-8 cabin indicate the RH is $\leq 40\%$

508 (Fig. S9), leading to sulfuric acid weight percentage of 50% or greater (Wilson, 1921).

509 Therefore, the accommodation coefficient of ~1 is well-constrained by the literature. Thus, the

510 handling of the filters between the sampling inlet to the Teflon bag exposes the acidic PM to

511 enough gas-phase ammonia towards forming ammonium bisulfate or ammonium sulfate, biasing

512 high ammonium from the filters. This explains the differences seen in Fig. 1 – Fig. 4.

513   Another potential limitation is that the PM on the filters could form a layer, as multiple

514 particles pile up on top of each other, slowing the diffusion of ammonia to be taken up by acidic

515 PM. The filters have a one-sided surface area of 6.4×10^{-3} m^2, while an individual particle at the

516 mode of the volume distribution (Fig. 7) has a projected surface area of ~7.1×10^{-14} m^2. Thus,

517 ~9.0×10^{10} particles would need to be collected to form a single layer of PM on the filter. The

518 number of molecules in a single particle of the mode size is ~1.4×10^{8} molecules (Eq. S2).

519 Therefore, ~1.3×10^{19} molecules need to be collected onto the filters in order to form a monolayer

520 of PM, which is equivalent to ~2.2×10^{3} μg total aerosol collected or ~700 μg sm^{-3} aerosol

521 concentration. As the mass concentration in ATom was typically ~1 μg sm^{-3} (Hodzic et al.,

522 2020), and total aerosol concentrations that high is rarely seen except for extreme events (such as

523 the thickest fresh wildfire plumes), it is very unlikely that more particle layering would delay the

524 diffusion of ammonia to acidic PM.

525   Various sensitivity analyses of the uptake of ammonia to sulfuric acid were conducted.

526 First, there is minimal impact of cabin temperature on the results. Though there was a 25 K range

527 in cabin temperature (Fig. S2), the impact on the molecular speed of ammonia in the model (Eq.

Atmospheric
Measurement
Techniques
Discussions
Open Access

EGU

528 S1) leads to a ±2% change in molecular speed, resulting in small changes in the time. Further,

529 only large changes in the accommodation coefficient with temperature occurs for sulfuric acid

530 weight percentages < 40% (Swartz et al., 1999), which is smaller than the weight percentage

531 expected for the filters in the cabin of the DC-8. For the temperature range of the cabin of the

532 DC-8 (Fig. S2), the coefficient changes by less than 10%, which leads to a total maximum

533 change in Fig. 7 of ±12%. The largest impact on the results in Fig. 7 is changing the

534 accommodation coefficient. Reducing the accommodation coefficient by a factor of 10, though

535 not representative of the DC-8 cabin conditions, would mean the acidic PM would need to be

536 exposed to ammonia for ≥ 1 minute (Fig. S10). It is expected that the lower accommodation

537 coefficient will occur for conditions with higher RH (>80%), suggesting typical laboratory

538 conditions (along with the lower ammonia mixing ratios) or ambient conditions may experience

539 lower ammonia uptake to acidic PM. Finally, organic coatings may impact the accommodation

540 coefficient of ammonia to sulfuric acid; however, the amount of reduction on the accommodation

541 coefficient has varied among studies (e.g., Daumer et al., 1992; Liggio et al., 2011). Daumer et

542 al. (1992) showed no impact; whereas, Liggio et al. (2011) found a similar impact to reducing the

543 accommodation coefficient by a factor of 10 (Fig. S10). Thus, the results in Fig. 7 are in line

544 with Daumer et al. (1992) while the results in Fig. S10 are in line with Liggio et al. (2011).

545

546 **3.4 Impacts of Ammonia Uptake on Acidic Filters**

547   As discussed throughout this study, uptake of cabin ammonia during the handling of

548 acidic filters can lead to biases in ammonium mass concentrations. However, other potential

549 sources of biases include the material used for sampling and storing the filter (Hayes et al.,

550 1980), and the preparation of the filter in the field to be sampled by ion chromatography. As the

551 preparation of the filters occurs indoors, as well, the filters will be exposed to similar ammonia

552 mixing ratios to those shown in Fig. 6.

553   Further, filter collection of aerosols is a widely used technique outside of aircraft

554 campaigns, including for regulatory purposes and long-term monitoring at various locations

555 around the world. For many of these sites, ammonia denuders are used to minimize biases of

556 ammonium on filters (e.g, (Baltensperger et al., 2003)). Data from remote, high altitude locations

557 have indicated that the ammonium balance is less than one (Cozic et al., 2008; Sun et al., 2009;

558 Freney et al., 2016; Zhou et al., 2019), similar to the observations from the AMS shown in Fig.

559 3. However, this is dependent on air mass origin and type (Cozic et al., 2008; Sun et al., 2009;

560 Fröhlich et al., 2015). Thus, sampling of remote aerosols with filters does provide evidence of

561 ammonium balances less than one due to a combination of procedures to minimize interaction of

562 gas-phase ammonia with the acidic filters and the lower human presence (and potentially cooler

563 temperatures at high, remote, mountaintop locations such as Jungfraujoch).

564   However, there are some long-term monitoring stations that do not use denuders or other

565 practices to minimize the interaction of ammonia with acidic aerosols. For example, the Clean

566 Air Status and Trends Network (CASTNET), which is located throughout the continental United

567 States, measures ammonium, sulfate, and nitrate (Solomon et al., 2014). The CASTNET system

568 uses an open-face system to collect aerosols on Teflon filters for approximately one week for

569 each filter (Lavery et al., 2009). In comparison, the Chemical Speciation Monitoring Network

570 (CSN), which also samples the continental United States and collects the aerosols on Nylon or

571 Teflon filters, a denuder is used to scrub gas-phase ammonia to minimize interaction of ammonia

572 with acidic aerosols on filters (Solomon et al., 2000, 2014). The comparison between these two

573 long-term monitoring sites show very different trends of ammonium balance versus total

574 inorganic mass concentration (Fig. S11). For CSN, the ammonium balance decreases with mass

575 concentration whereas CASTNET remains nearly constant. This is similar to the comparison

576 between SAGA and AMS in Fig. 4. This difference between the two sampling techniques may

577 be due to the lack of denuder in CASTNET to remove gas-phase ammonia. The use of the

578 denuders has led to CSN and other monitoring networks that use denuders to be more in-line

579 with in-situ observations (Kim et al., 2015; Weber et al., 2016). Further, as shown in Fig. S8,

580 exposure of an unprotected acidic filter for time greater than 1 day will lead to ammonia reacting

581 with the acid to form ammonium bisulfate or ammonium sulfate, even at low ammonia mixing

582 ratios. Thus, without denuders, or handling of filters with more than one person present, will lead

583 to similar differences between in-situ sampling versus filter collection of inorganic aerosols

584 observed during various aircraft campaigns.

585   Further, the uptake of ammonia onto acidic aerosols will impact comparisons with

586 chemical transport models (CTMs) and the understanding of various physical processes. For

587 example, various CTMs predict different results for the mass concentration of ammonium in the

588 upper troposphere (Wang et al., 2008a; Fisher et al., 2011; Ge et al., 2018), and selection of one

589 measurement versus the other will lead to different degrees of agreement. For example, for filters

590 that collect aerosols similar to those described here (no ammonia scrubber and/or exposed to

591 human emissions of ammonia), values of ammonium $< 0.2\ \mu g\ m^{-3}$ should not be used and either

592 disregarded or instead use *on-line* measurements of ammonium. This different agreement

593 impacts our understanding of important processes, such as the direct radiative impact of

Atmospheric
Measurement
Techniques
Discussions

594 inorganic aerosol (Wang et al., 2008b) or deposition of inorganic gases and aerosols (Nenes et

595 al., 2020a), as the gas-phase species have a faster deposition rate than the aerosol-phase. Finally,

596 the measurement biases can impact the suggested regulations to improve air quality (Nenes et al.,

597 2020b) and the calculated aerosol pH, as the pH is sensitive to the partitioning of ammonia

598 between the aerosol- and gas-phase (e.g., Hennigan et al., 2015).

599

600 **Conclusions**

601   Collection of aerosols onto filters to measure aerosol mass concentration and composition

602 is valuable for improving our understanding of the emissions and chemistry of inorganic aerosol,

603 and longstanding, multi-decadal filter-based records of atmospheric composition are invaluable

604 to analyze atmospheric change. However, as had been discussed in earlier studies, acidic aerosols

605 collected on filters are susceptible to uptake of gas-phase ammonia, which interacts with the

606 acidic aerosol to form an ammonium salt (e.g., ammonium bisulfate or ammonium sulfate). This

607 artifact in filter measurements can bias our understanding on the chemical composition of the

608 aerosol, which impacts numerous atmospheric processes.

609   We show that across six different aircraft campaigns, the aerosol collected on filters

610 showed a substantially higher ammonium mass concentration and ammonium balance compared

611 to AMS measurements. Further, another *on-line* measurement (PALMS) also shows lower

612 ammonium-to-sulfate ratios than for the filters. These differences are not due to differences in

613 the aerosol size ranges sampled by the PALMS and the filters. Instead, we show that the mixing

614 ratio of gas-phase ammonia in the cabin of the DC-8 is high enough (mean ~45 ppbv), and

615 similar to other indoor environments, to interact with acidic aerosol collected on filters in ≤ 10 s,

Atmospheric
Measurement
Techniques
Discussions

Open Access
EGU

616 to form ammonium salts. These results are consistent with prior studies investigating this

617 interference. Thus, due to the interaction of ammonia in the cabin of research aircraft, we suggest

618 that a more realistic limit-of-detection of ammonium is 200 ng sm^{-3}, versus the 10 ng sm^{-3}

619 typically cited based on the ion chromatography measurement. Finally, even though methods to

620 reduce this bias have been implemented in several ground-based long-term filter measurements

621 of inorganic aerosols, there are still some networks that collect inorganic aerosol without

622 denuders to remove gas-phase ammonia, leading to similar discrepancies between ground

623 networks as observed between filters and AMS on the various aircraft campaigns. Careful

624 practice in both the aerosol collection and filtering handling is necessary to better understand the

625 emissions, chemistry, and chemical and physical properties of inorganic aerosol.

626

Acknowledgements

628

640

Data Availability

642

643   ARCTAS-A   and   -B   measurements   are   available   at
644 http://doi.org/10.5067/SUBORBITAL/ARCTAS2008/DATA001, last access 27 April 2020.
645 SEAC^{4}RS   measurements   are   available   at
646 http://doi.org/10.5067/Aircraft/SEAC4RS/Aerosol-TraceGas-Cloud, last access 27 April 2020.
647 WINTER measurements are available at https://data.eol.ucar.edu/master_lists/generated/winter/,
648 last access 27 April 2020. ATom-1 and -2 measurements are available at
649 https://doi.org/10.3334/ORNLDAAC/1581, last access 27 April 2020. Ammonia and carbon
650 dioxide measurements from the cabin of the DC-8 are available as an attachment . CSN and

651   CASTNET   measurements   are   available   at

652   http://views.cira.colostate.edu/fed/QueryWizard/Default.aspx, last access 27 April 2020.

653 **Figures**

654
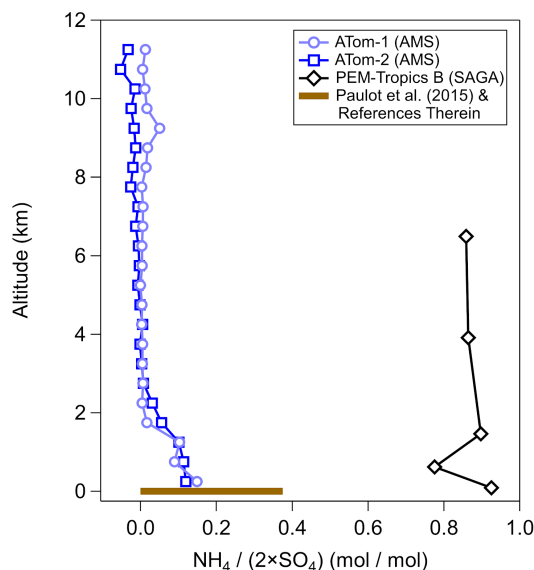
655 Figure 1. *Vertical profile of sulfate-only ion molar balance (moles(NH$_4$)/moles(SO$_4$)) measured*
656 *during PEM-Tropics by collecting the aerosol on filters and analyzing it off-line with ion*
657 *chromatography (Dibb et al., 2002) and during ATom-1 and -2 by AMS (Hodzic et al., 2020).*
658 *The ammonium balance profile is for observations collected during ATom-1 and -2 between*
659 *-20°S and 20°N in the Pacific basin, so that the observations were in a similar location as the*
660 *PEM-Tropics samples. Also shown is the ammonium balance from observations summarized in*
661 *Paulot et al. (2015), and reference therein, for the area around the same location as*
662 *PEM-Tropics.*
663

664
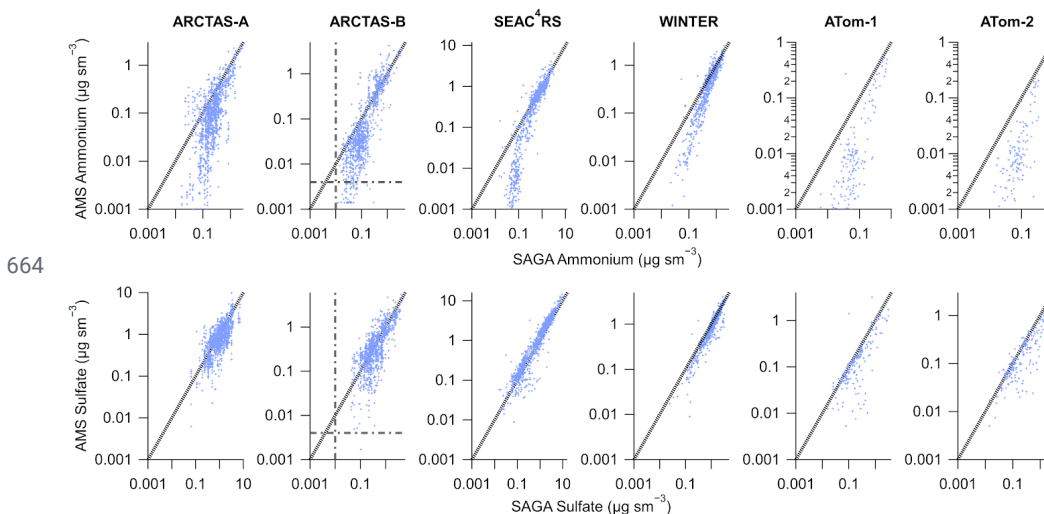
Figure 2. *Scatter plot of AMS (y-axis) versus SAGA filter (x-axis) ammonium (top) and sulfate (bottom) mass concentration from 6 different aircraft campaigns. AMS data have been averaged over the SAGA filter collection times. Black line is the one-to-one line and the grey dash-dot lines are the estimated detection limits for AMS (DeCarlo et al., 2006; Guo et al., 2020) at the SAGA filter collection interval (~5 minutes) and the estimated detection limits for SAGA (Dibb et al., 1999). Data has been averaged to the sampling time of SAGA and has not been filtered for supermicron particles. For ATom-1 and -2, data during ascent and descent has been removed (only level sampling at low altitude and high altitude).*

Figure 3. *Vertical profiles of ammonium balance* $((NH_4/18)/(2 \times SO_4/96 + NO_3/62))$ *for (a) ARCTAS-A, (b) ARCTAS-B, (c) SEAC^{4}RS, (d) WINTER, (e) ATom-1, and (f) ATom-2, for AMS and SAGA. The binned data is the mean for each 100 hPa pressure level. The data has been averaged to the sampling time of SAGA filters.*

678
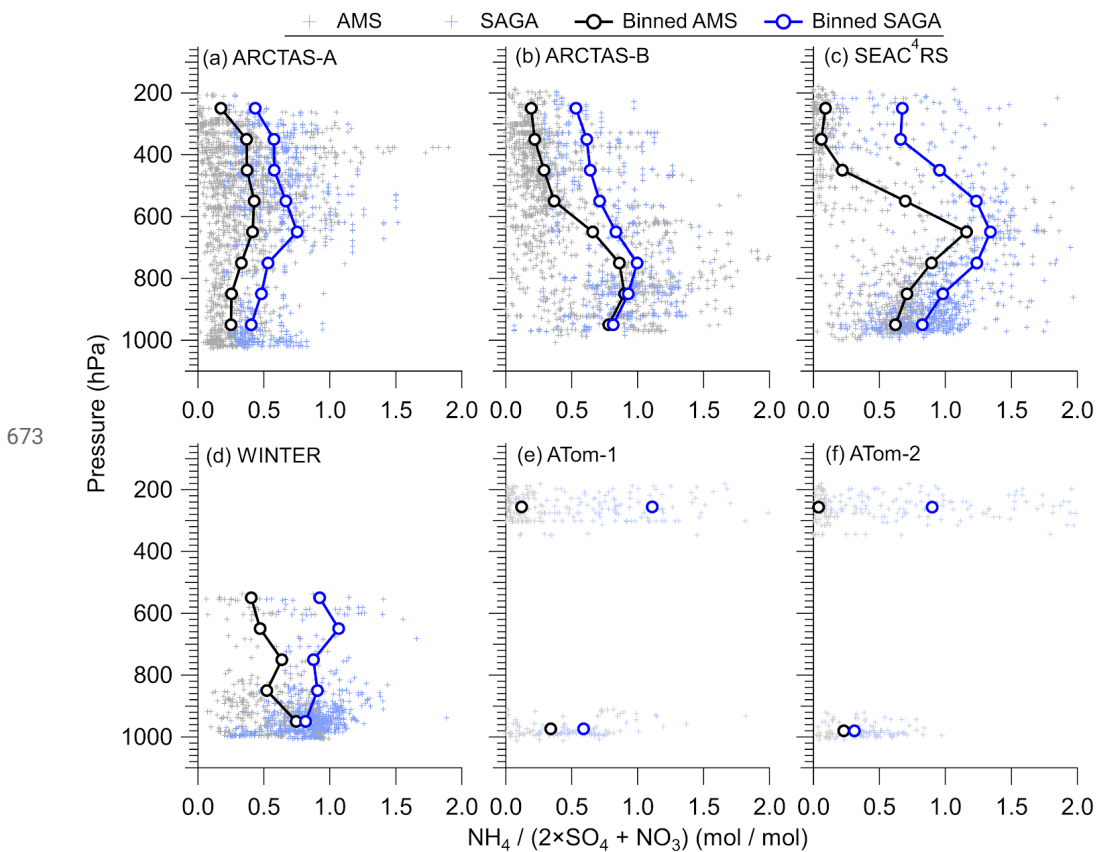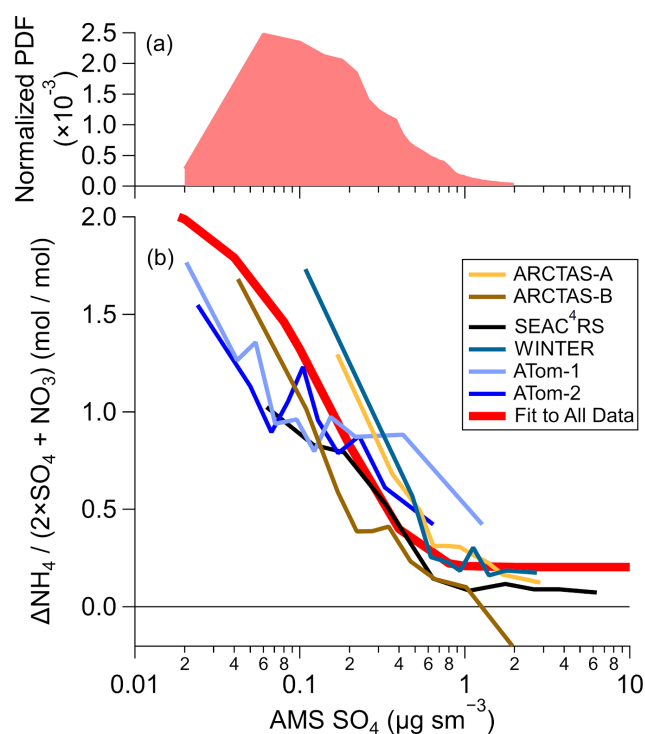
680 Figure 4. *(a) Predicted normalized probability distribution function (PDF) for tropospheric*
681 *(pressure > 250 hPa) sulfate from GEOS-Chem for one model year (see SI). (b) Difference*
682 *between SAGA and AMS ammonium, in mol sm⁻³, divided by AMS sulfate and nitrate, in mol*
683 *sm⁻³, versus AMS sulfate (μg sm⁻³), for the six different airborne campaigns. The values shown*
684 *are binned deciles for the five different airborne campaigns. The fit shown in (b) is for all data*
685 *from all campaigns.*
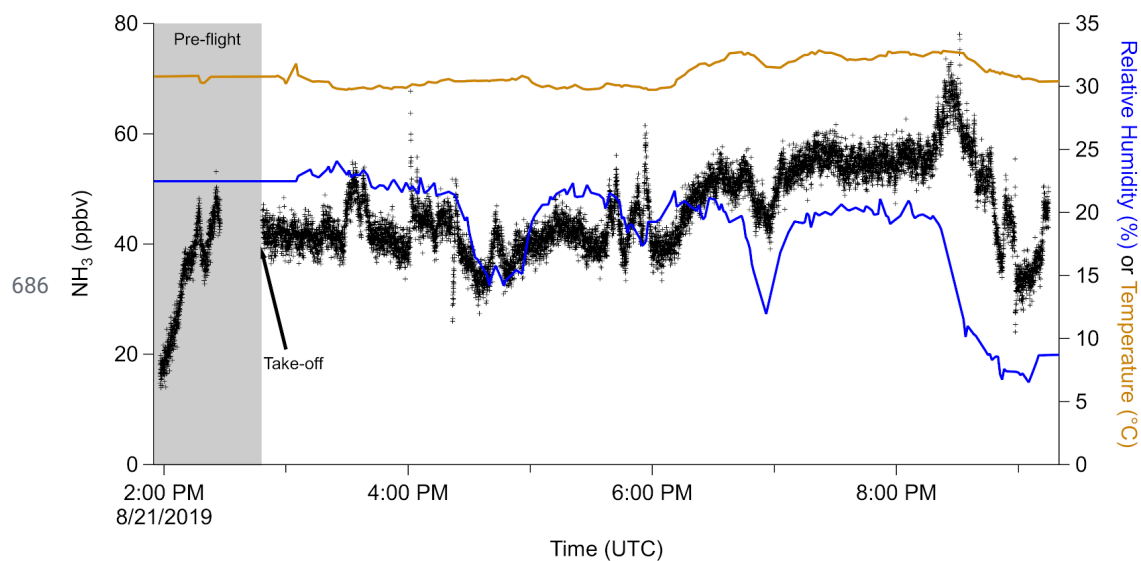
Figure 5. *Time series of ammonia (left) and relative humidity and temperature (right) measured inside the cabin of the NASA DC-8 during a flight during the FIREX-AQ campaign. Time spent prior to take-off is marked with a grey background.*
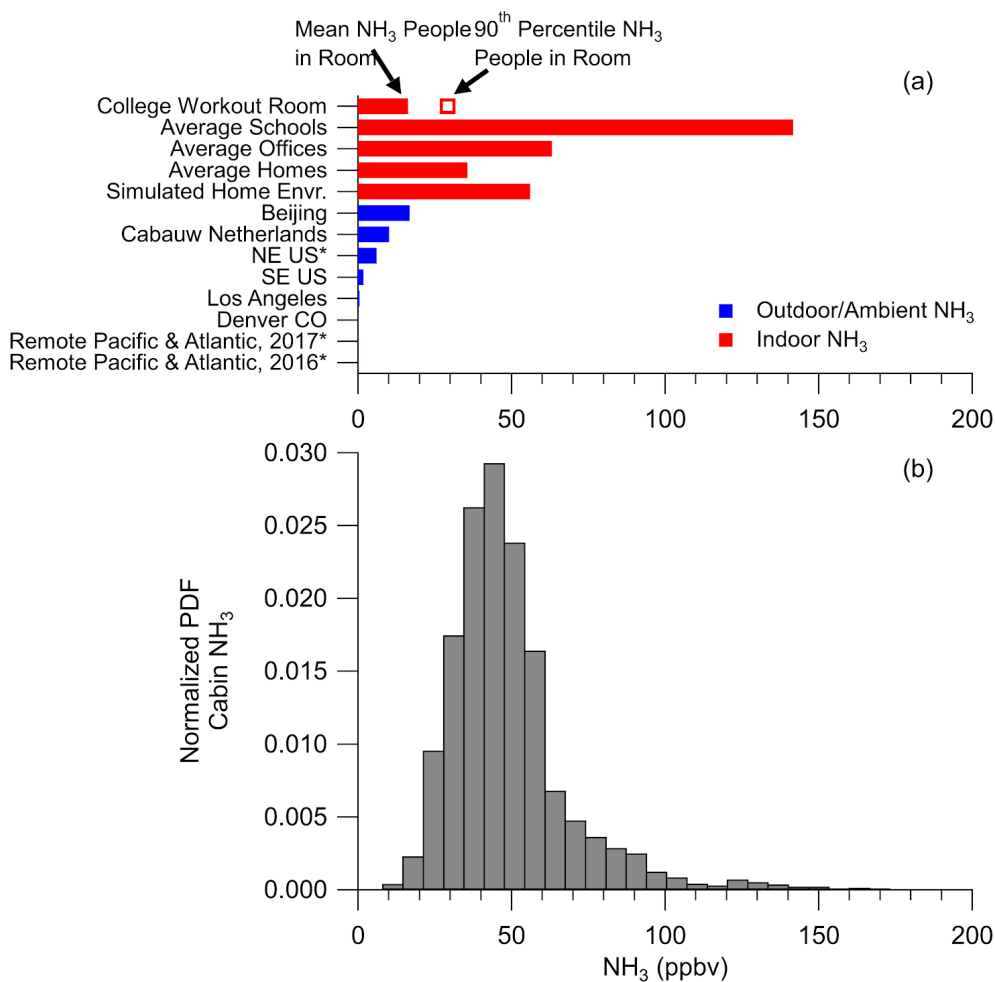
Figure 6. *(a) Ammonia (NH₃) (ppbv) reported for studies. See* Table S1 *for references. Asterisk after study name indicates NH₃ predicted by thermodynamic model instead of being measured. (b) Normalized probability distribution function (PDF) for NH₃, measured in the cabin of the NASA DC-8 during FIREX-AQ.*
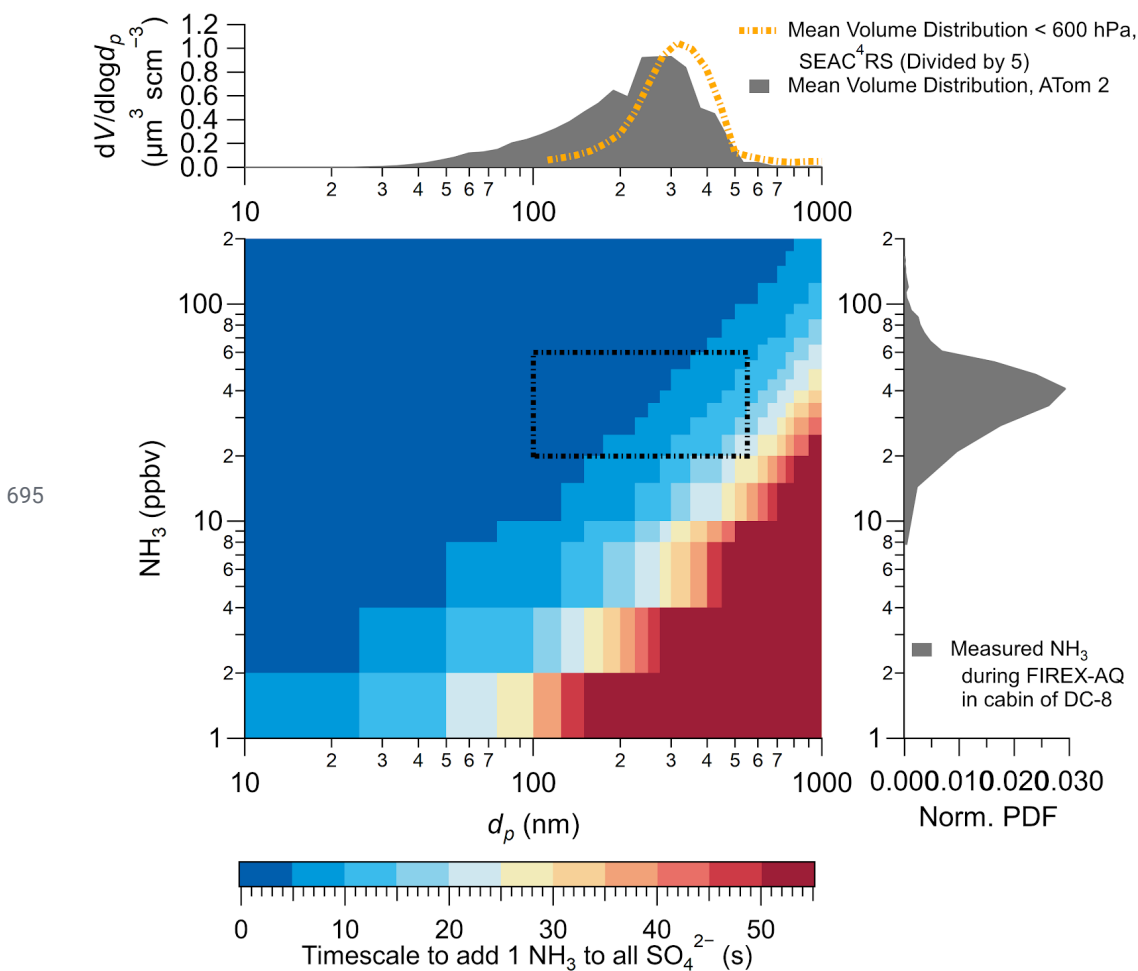
Figure 7. *Theoretical calculation for the amount of time it would take for all the sulfuric acid on the filter to react with one ammonia molecule to become ammonium bisulfate. Volume distribution is the average from SEAC⁴RS and ATom-2 (adapted from Guo et al. (2020)) and the normalized probability distribution function (Norm. PDF) is from* Fig. 6. *The representative diameter and ammonia mixing ratio are shown as dashed lines in the calculated timescale.*

Atmospheric
Measurement
Techniques
Discussions

Open Access

EGU

References

701 **References**

702 Abbatt, J. P. D., Benz, S., Cziczo, D. J., Kanji, Z., Lohmann, U. and Möhler, O.: Solid
703 ammonium sulfate aerosols as ice nuclei: a pathway for cirrus cloud formation, Science,
704 313(5794), 1770–1773, 2006.

705 Ampollini, L., Katz, E. F., Bourne, S., Tian, Y., Novoselac, A., Goldstein, A. H., Lucic, G.,
706 Waring, M. S. and DeCarlo, P. F.: Observations and Contributions of Real-Time Indoor
707 Ammonia Concentrations during HOMEChem, Environ. Sci. Technol., 53(15), 8591–8598,
708 2019.

709 Bahreini, R., Dunlea, E. J., Matthew, B. M., Simons, C., Docherty, K. S., DeCarlo, P. F., Jimenez,
710 J. L., Brock, C. A. and Middlebrook, A. M.: Design and Operation of a Pressure-Controlled Inlet
711 for Airborne Sampling with an Aerodynamic Aerosol Lens, Aerosol Sci. Technol., 42(6),
712 465–471, 2008.

713 Bahreini, R., Ervens, B., Middlebrook, A. M., Warneke, C., De Gouw, J. A., DeCarlo, P. F.,
714 Jimenez, J. L., Brock, C. A., Neuman, J. A., Ryerson, T. B., Stark, H., Atlas, E., Brioude, J.,
715 Fried, A., Holloway, J. S., Peischl, J., Richter, D., Walega, J., Weibring, P., Wollny, A. G. and
716 Fehsenfeid, F. C.: Organic aerosol formation in urban and industrial plumes near Houston and
717 Dallas, Texas, J. Geophys. Res. D: Atmos., 114(16), 1–17, 2009.

718 Baltensperger, U., Barrie, L., Frohlich, C., Gras, J., Jager, H., Jennings, S. G., Li, S.-M., Ogren,
719 J., Widensohler, A., Wehrli, C. and Wilson, J.: WMO/GAW Aerosol Measurement Procedures
720 Guidelines and Recommendations, WMO GAW. [online] Available from:
721 https://library.wmo.int/doc_num.php?explnum_id=9244, 2003.

722 von Bobrutzki, K., Braban, C. F., Famulari, D., Jones, S. K., Blackall, T., Smith, T. E. L., Blom,
723 M., Coe, H., Gallagher, M., Ghalaieny, M., McGillen, M. R., Percival, C. J., Whitehead, J. D.,
724 Ellis, R., Murphy, J., Mohacsi, A., Pogany, A., Junninen, H., Rantanen, S., Sutton, M. A. and
725 Nemitz, E.: Field inter-comparison of eleven atmospheric ammonia measurement techniques,
726 Atmos. Meas. Tech., 3(1), 91–112, 2010.

727 Brock, C. A., Williamson, C., Kupc, A., Froyd, K. D., Erdesz, F., Wagner, N., Richardson, M.,
728 Schwarz, J. P., Gao, R.-S., Katich, J. M., Campuzano-Jost, P., Nault, B. A., Schroder, J. C.,
729 Jimenez, J. L., Weinzierl, B., Dollner, M., Bui, T. and Murphy, D. M.: Aerosol size distributions
730 during the Atmospheric Tomography Mission (ATom): methods, uncertainties, and data products,
731 Atmos. Meas. Tech., 12(6), 3081–3099, 2019.

732 Brundrett, G.: Comfort and health in commercial aircraft: a literature review, J. R. Soc. Promot.
733 Health, 121(1), 29–37, 2001.

734 Canagaratna, M. R., Jayne, J. T., Jimenez, J. L., Allan, J. D., Alfarra, M. R., Zhang, Q., Onasch,
735 T. B., Drewnick, F., Coe, H., Middlebrook, A., Delia, A., Williams, L. R., Trimborn, A. M.,
736 Northway, M. J., DeCarlo, P. F., Kolb, C. E., Davidovits, P. and Worsnop, D. R.: Chemical and
737 microphysical characterization of ambient aerosols with the aerodyne aerosol mass spectrometer,

Atmospheric
Measurement
Techniques
Discussions

738 Mass Spectrom. Rev., 26(2), 185–222, 2007.

739 Cheng, Y. and He, K.-B.: Measurement of carbonaceous aerosol with different sampling
740 configurations and frequencies, Atmospheric Measurement Techniques, 8(7), 2639–2648, 2015.

741 Chow, J. C., Watson, J. G., Lowenthal, D. H. and Magliano, K. L.: Loss of PM $_{2.5}$ Nitrate from
742 Filter Samples in Central California, J. Air Waste Manage. Assoc., 55(8), 1158–1168, 2005.

743 Chow, J. C., Watson, J. G., Chen, L.-W. A., Rice, J. and Frank, N. H.: Quantification of $PM_{2.5}$
744 organic carbon sampling artifacts in US networks, Atmos. Chem. Phys., 10(12), 5223–5239,
745 2010.

746 Clark, K. W., Anderson, K. R., Linn, W. S. and Gong, H., Jr: Influence of breathing-zone
747 ammonia on human exposures to acid aerosol pollution, J. Air Waste Manag. Assoc., 45(11),
748 923–925, 1995.

749 Cohen, A. J., Brauer, M., Burnett, R., Anderson, H. R., Frostad, J., Estep, K., Balakrishnan, K.,
750 Brunekreef, B., Dandona, L., Dandona, R., Feigin, V., Freedman, G., Hubbell, B., Jobling, A.,
751 Kan, H., Knibbs, L., Liu, Y., Martin, R., Morawska, L., Pope, C. A., Shin, H., Straif, K.,
752 Shaddick, G., Thomas, M., van Dingenen, R., van Donkelaar, A., Vos, T., Murray, C. J. L. and
753 Forouzanfar, M. H.: Estimates and 25-year trends of the global burden of disease attributable to
754 ambient air pollution: an analysis of data from the Global Burden of Diseases Study 2015,
755 Lancet, 389(10082), 1907–1918, 2017.

756 Colberg, C. A., Luo, B. P., Wernli, H., Koop, T. and Peter, T.: A novel model to predict the
757 physical state of atmospheric $H_2SO_4/NH_3/H_2O$ aerosol particles, Atmos. Chem. Phys., 3(4),
758 909–924, 2003.

759 Coury, C. and Dillner, A. M.: ATR-FTIR characterization of organic functional groups and
760 inorganic ions in ambient aerosols at a rural site, Atmos. Environ., 43(4), 940–948, 2009.

761 Cozic, J., Verheggen, B., Weingartner, E., Crosier, J., Bower, K. N., Flynn, M., Coe, H.,
762 Henning, S., Steinbacher, M., Henne, S., Collaud Coen, M., Petzold, A. and Baltensperger, U.:
763 Chemical composition of free tropospheric aerosol for PM_1 and coarse mode at the high alpine
764 site Jungfraujoch, Atmos. Chem. Phys., 8(2), 407–423, 2008.

765 Cubison, M. J., Ortega, A. M., Hayes, P. L., Farmer, D. K., Day, D. A., Lechner, M. J., Brune, W.
766 H., Apel, E., Diskin, G. S., Fisher, J. A., Fuelberg, H. E., Hecobian, A., Knapp, D. J., Mikoviny,
767 T., Riemer, D., Sachse, G. W., Sessions, W., Weber, R. J., Weinheimer, A. J., Wisthaler, A. and
768 Jimenez, J. L.: Effects of aging on organic aerosol from open biomass burning smoke in aircraft
769 and laboratory studies, Atmos. Chem. Phys., 11(23), 12049–12064, 2011.

770 Daumer, B., Niessner, R. and Klockow, D.: Laboratory studies of the influence of thin organic
771 films on the neutralization reaction of H_2SO_4 aerosol with ammonia, J. Aerosol Sci., 23(4),
772 315–325, 1992.

773 DeCarlo, P. F., Kimmel, J. R., Trimborn, A., Northway, M. J., Jayne, J. T., Aiken, A. C., Gonin,

774 M., Fuhrer, K., Horvath, T., Docherty, K. S., Worsnop, D. R. and Jimenez, J. L.:
775 Field-deployable, high-resolution, time-of-flight aerosol mass spectrometer, Anal. Chem.,
776 78(24), 8281–8289, 2006.

777 DeCarlo, P. F., Dunlea, E. J., Kimmel, J. R., Aiken, A. C., Sueper, D., Crounse, J., Wennberg, P.
778 O., Emmons, L., Shinozuka, Y., Clarke, A., Zhou, J., Tomlinson, J., Collins, D. R., Knapp, D.,
779 Weinheimer, A. J., Montzka, D. D., Campos, T. and Jimenez, J. L.: Fast airborne aerosol size and
780 chemistry measurements above Mexico City and Central Mexico during the MILAGRO
781 campaign, Atmos. Chem. Phys., 8(14), 4027–4048, 2008.

782 Dentener, F. J. and Crutzen, P. J.: A three-dimensional model of the global ammonia cycle, J.
783 Atmos. Chem., 19(4), 331–369, 1994.

784 Dibb, J. E., Talbot, R. W., Scheuer, E. M., Blake, D. R., Blake, N. J., Gregory, G. L., Sachse, G.
785 W. and Thornton, D. C.: Aerosol chemical composition and distribution during the Pacific
786 Exploratory Mission (PEM) Tropics, J. Geophys. Res., 104(D5), 5785–5800, 1999.

787 Dibb, J. E., Talbot, R. W. and Scheuer, E. M.: Composition and distribution of aerosols over the
788 North Atlantic during the Subsonic Assessment Ozone and Nitrogen Oxide Experiment
789 (SONEX), J. Geophys. Res. D: Atmos., 105(D3), 3709–3717, 2000.

790 Dibb, J. E., Talbot, R. W., Seid, G., Jordan, C., Scheuer, E., Atlas, E., Blake, N. J. and Blake, D.
791 R.: Airborne sampling of aerosol particles: Comparison between surface sampling at Christmas
792 Island and P-3 sampling during PEM-Tropics B, J. Geophys. Res., 108(D2), 11335, 2002.

793 Dibb, J. E., Talbot, R. W., Scheuer, E. M., Seid, G., Avery, M. A. and Singh, H. B.: Aerosol
794 chemical composition in Asian continental outflow during the TRACE-P campaign: Comparison
795 with PEM-West B, J. Geophys. Res.: Atmos., 108(D21), 8815, 2003.

796 Dzepina, K., Arey, J., Marr, L. C., Worsnop, D. R., Salcedo, D., Zhang, Q., Onasch, T. B.,
797 Molina, L. T., Molina, M. J. and Jimenez, J. L.: Detection of particle-phase polycyclic aromatic
798 hydrocarbons in Mexico City using an aerosol mass spectrometer, Int. J. Mass Spectrom., 263(2),
799 152–170, 2007.

800 Faloona, I.: Sulfur processing in the marine atmospheric boundary layer: A review and critical
801 assessment of modeling uncertainties, Atmos. Environ., 43(18), 2841–2854, 2009.

802 Filges, A., Gerbig, C., Rella, C. W., Hoffnagle, J., Smit, H., Krämer, M., Spelten, N., Rolf, C.,
803 Bozóki, Z., Buchholz, B. and Ebert, V.: Evaluation of the IAGOS-Core GHG package H$_2$O
804 measurements during the DENCHAR airborne inter-comparison campaign in 2011, Atmos.
805 Meas. Tech., 11(9), 5279–5297, 2018.

806 Finewax, Z., Pagonis, D., Claflin, M. S., Handschy, A. V., Brown, W. L., Ba, J. O. N., Lerner, B.
807 M., Jimenez, J. L., Ziemann, P. J. and de Gouw, J. A.: Quantification and source characterization
808 of volatile organic compounds from exercising and application of chlorine-based cleaning
809 products in a university athletic center, Indoor Air, Submitted, 2020.

40

810 Fisher, J. A., Jacob, D. J., Wang, Q., Bahreini, R., Carouge, C. C., Cubison, M. J., Dibb, J. E.,
811 Diehl, T., Jimenez, J. L., Leibensperger, E. M., Lu, Z., Meinders, M. B. J., Pye, H. O. T., Quinn,
812 P. K., Sharma, S., Streets, D. G., van Donkelaar, A. and Yantosca, R. M.: Sources, distribution,
813 and acidity of sulfate–ammonium aerosol in the Arctic in winter–spring, Atmos. Environ.,
814 45(39), 7301–7318, 2011.

815 Freney, E., Sellegri Karine, S. K., Eija, A., Clemence, R., Aurelien, C., Jean-Luc, B., Aurelie, C.,
816 Hervo Maxime, H. M., Nadege, M., Laeticia, B. and David, P.: Experimental Evidence of the
817 Feeding of the Free Troposphere with Aerosol Particles from the Mixing Layer, Aerosol Air
818 Qual. Res., 16(3), 702–716, 2016.

819 Fröhlich, R., Cubison, M. J., Slowik, J. G., Bukowiecki, N., Canonaco, F., Croteau, P. L., Gysel,
820 M., Henne, S., Herrmann, E., Jayne, J. T., Steinbacher, M., Worsnop, D. R., Baltensperger, U.
821 and Prévôt, A. S. H.: Fourteen months of on-line measurements of the non-refractory submicron
822 aerosol at the Jungfraujoch (3580 m a.s.l.) – chemical composition, origins and organic aerosol
823 sources, Atmos. Chem. Phys., 15(19), 11373–11398, 2015.

824 Froyd, K. D., Murphy, D. M., Sanford, T. J., Thomson, D. S., Wilson, J. C., Pfister, L. and Lait,
825 L.: Aerosol composition of the tropical upper troposphere, Atmos. Chem. Phys., 9(13),
826 4363–4385, 2009.

827 Froyd, K. D., Murphy, D. M., Brock, C. A., Campuzano-Jost, P., Dibb, J. E., Jimenez, J.-L.,
828 Kupc, A., Middlebrook, A. M., Schill, G. P., Thornhill, K. L., Williamson, C. J., Wilson, J. C.
829 and Ziemba, L. D.: A new method to quantify mineral dust and other aerosol species from
830 aircraft platforms using single-particle mass spectrometry, Atmos. Meas. Tech., 12(11),
831 6209–6239, 2019.

832 Fuchs, N. A. and Sutugin, A. G.: High-Dispersed Aerosols, in Topics in Current Aerosol
833 Research, edited by G. M. Hidy and J. R. Brock, Pergamon., 1971.

834 Ge, C., Zhu, C., Francisco, J. S., Zeng, X. C. and Wang, J.: A molecular perspective for global
835 modeling of upper atmospheric NH3 from freezing clouds, Proc. Natl. Acad. Sci. U. S. A.,
836 115(24), 6147–6152, 2018.

837 Guo, H., Xu, L., Bougiatioti, A., Cerully, K. M., Capps, S. L., Hite, J. R., Carlton, A. G., Lee,
838 S.-H., Bergin, M. H., Ng, N. L., Nenes, A. and Weber, R. J.: Fine-particle water and pH in the
839 southeastern United States, Atmos. Chem. Phys., 15(9), 5211–5228, 2015.

840 Guo, H., Nenes, A. and Weber, R. J.: The underappreciated role of nonvolatile cations in aerosol
841 ammonium-sulfate molar ratios, Atmos. Chem. Phys., 18(23), 17307–17323, 2018.

842 Guo, H., Campuzano-Jost, P., Nault, B. A., Day, D. A., Schroder, J. C., Williamson, C., Kupc,
843 A., Brock, C. A., Froyd, K. D., Murphy, D. M., Katich, J. M., Dibb, J. E., Dollner, M., Weinzierl,
844 B. and Jimenez, J. L.: The Importance of Size Ranges in Intercomparison of Aerosol Volume
845 Concentration Measurements: A Case Study for Aerosol Mass Spectrometer in the ATom
846 Mission, Atmos. Meas. Tech. Discuss., Submitted, 2020.

Atmospheric
Measurement
Techniques
Discussions

Open Access

EGU

847 Hanson, D. and Kosciuch, E.: The NH_3 Mass Accommodation Coefficient for Uptake onto
848 Sulfuric Acid Solutions, J. Phys. Chem. A, 107(13), 2199–2208, 2003.

849 Hanson, D. R. and Kosciuch, E.: Reply to "Comment on 'The NH_3 Mass Accommodation
850 Coefficient for Uptake onto Sulfuric Acid Solutions,'" J. Phys. Chem. A, 108(40), 8549–8551,
851 2004.

852 Hayes, D., Snetsinger, K., Ferry, G., Oberbeck, V. and Farlow, N.: Reactivity of stratospheric
853 aerosols to small amounts of ammonia in the laboratory environment, Geophys. Res. Lett., 7(11),
854 974–976, 1980.

855 Heald, C. L. and Kroll, J. H.: The fuel of atmospheric chemistry: Toward a complete description
856 of reactive organic carbon, Sci Adv, 6(6), eaay8967, 2020.

857 Heald, C. L., Collett, J. L., Jr., Lee, T., Benedict, K. B., Schwandner, F. M., Li, Y., Clarisse, L.,
858 Hurtmans, D. R., Van Damme, M., Clerbaux, C., Coheur, P.-F., Philip, S., Martin, R. V. and Pye,
859 H. O. T.: Atmospheric ammonia and particulate inorganic nitrogen over the United States,
860 Atmos. Chem. Phys., 12(21), 10295–10312, 2012.

861 Heim, E. W., Dibb, J., Scheuer, E., Jost, P. C., Nault, B. A., Jimenez, J. L., Peterson, D., Knote,
862 C., Fenn, M., Hair, J., Beyersdorf, A. J., Corr, C. and Anderson, B. E.: Asian dust observed
863 during KORUS-AQ facilitates the uptake and incorporation of soluble pollutants during transport
864 to South Korea, Atmos. Environ., 224, 117305, 2020.

865 Hennigan, C. J., Sullivan, A. P., Fountoukis, C. I., Nenes, A., Hecobian, A., Vargas, O., Peltier,
866 R. E., Hanks, A. T. C., Huey, L. G., Lefer, B. L., Russell, A. G. and Weber, R. J.: On the
867 volatility and production mechanisms of newly formed nitrate and water soluble organic aerosol
868 in Mexico City, Atmos. Chem. Phys., 8(14), 3761–3768, 2008.

869 Hennigan, C. J., Izumi, J., Sullivan, A. P., Weber, R. J. and Nenes, A.: A critical evaluation of
870 proxy methods used to estimate the acidity of atmospheric particles, Atmos. Chem. Phys., 15(5),
871 2775–2790, 2015.

872 Henze, D. K., Seinfeld, J. H. and Shindell, D. T.: Inverse modeling and mapping US air quality
873 influences of inorganic PM2.5 precursor emissions using the adjoint of GEOS-Chem, Atmos.
874 Chem. Phys., 9(16), 5877–5903, 2009.

875 Hering, S. and Cass, G.: The Magnitude of Bias in the Measurement of PM25 Arising from
876 Volatilization of Particulate Nitrate from Teflon Filters, J. Air Waste Manag. Assoc., 49(6),
877 725–733, 1999.

878 Hocking, M. B.: Indoor air quality: recommendations relevant to aircraft passenger cabins, Am.
879 Ind. Hyg. Assoc. J., 59(7), 446–454, 1998.

880 Hodzic, A. and Duvel, J. P.: Impact of Biomass Burning Aerosols on the Diurnal Cycle of
881 Convective Clouds and Precipitation Over a Tropical Island: Fire aerosols effect on deep

882 convection, J. Geophys. Res. D: Atmos., 123(2), 1017–1036, 2018.

883 Hodzic, A., Campuzano-Jost, P., Bian, H., Chin, M., Colarco, P. R., Day, D. A., Froyd, K. D.,
884 Heinold, B., Jo, D. S., Katich, J. M., Kodros, J. K., Nault, B. A., Pierce, J. R., Ray, E., Schacht,
885 J., Schill, G. P., Schroder, J. C., Schwarz, J. P., Sueper, D. T., Tegen, I., Tilmes, S., Tsigaridis, K.,
886 Yu, P. and Jimenez, J. L.: Characterization of Organic Aerosol across the Global Remote
887 Troposphere: A comparison of ATom measurements and global chemistry models, Atmos.
888 Chem. Phys., 20(8), 4607–4635, 2020.

889 Hunt, E. W. and Space, D. R.: The Airplane Cabin Environment: Issues Pertaining to Flight
890 Attendant, in Comfort," International in-flight Service Management Organization Conference.
891 [online]   Available   from:
892 http://citeseerx.ist.psu.edu/viewdoc/similar?doi=10.1.1.304.7321&type=cc (Accessed 25 March
893 2020), 1994.

894 Huntzicker, J. J., Cary, R. A. and Ling, C.-S.: Neutralization of sulfuric acid aerosol by ammonia,
895 Environ. Sci. Technol., 14(7), 819–824, 1980.

896 Hu, W., Hu, M., Hu, W., Jimenez, J. L., Yuan, B., Chen, W., Wang, M., Wu, Y., Chen, C., Wang,
897 Z., Peng, J., Zeng, L. and Shao, M.: Chemical composition, sources, and aging process of
898 submicron aerosols in Beijing: Contrast between summer and winter, J. Geophys. Res. D:
899 Atmos., 121(4), 1955–1977, 2016.

900 Hu, W., Campuzano-Jost, P., Day, D. A., Croteau, P., Canagaratna, M. R., Jayne, J. T., Worsnop,
901 D. R. and Jimenez, J. L.: Evaluation of the new capture vaporizer for aerosol mass spectrometers
902 (AMS) through field studies of inorganic species, Aerosol Sci. Technol., 51(6), 735–754, 2017a.

903 Hu, W., Campuzano-Jost, P., Day, D. A., Croteau, P., Canagaratna, M. R., Jayne, J. T., Worsnop,
904 D. R. and Jimenez, J. L.: Evaluation of the new capture vapourizer for aerosol mass
905 spectrometers (AMS) through laboratory studies of inorganic species, Atmospheric Measurement
906 Techniques, 10(6), 2897–2921, 2017b.

907 Hu, W., Campuzano-Jost, P., Day, D. A., Nault, B. A., Park, T., Lee, T., Pajunoja, A., Virtanen,
908 A., Croteau, P., Canagaratna, M. R., Jayne, J. T., Worsnop, D. R. and Jimenez, J. L.: Ambient
909 Quantification and Size Distributions for Organic Aerosol in Aerosol Mass Spectrometers with
910 the New Capture Vaporizer, ACS Earth Space Chem., doi:10.1021/acsearthspacechem.9b00310,
911 2020.

912 Jacob, D. J., Crawford, J. H., Maring, H., Clarke, A. D., Dibb, J. E., Emmons, L. K., Ferrare, R.
913 A., Hostetler, C. A., Russell, P. B., Singh, H. B., Thompson, A. M., Shaw, G. E., McCauley, E.,
914 Pederson, J. R. and Fisher, J. A.: The Arctic Research of the Composition of the Troposphere
915 from Aircraft and Satellites (ARCTAS) mission: design, execution, and first results, Atmos.
916 Chem. Phys., 10(11), 5191–5212, 2010.

917 Jimenez, J. L., Canagaratna, M. R., Donahue, N. M., Prevot, A. S. H., Zhang, Q., Kroll, J. H.,
918 DeCarlo, P. F., Allan, J. D., Coe, H., Ng, N. L., Aiken, A. C., Docherty, K. S., Ulbrich, I. M.,

Atmospheric
Measurement
Techniques
Discussions

919 Grieshop, A. P., Robinson, A. L., Duplissy, J., Smith, J. D., Wilson, K. R., Lanz, V. A., Hueglin,
920 C., Sun, Y. L., Tian, J., Laaksonen, A., Raatikainen, T., Rautiainen, J., Vaattovaara, P., Ehn, M.,
921 Kulmala, M., Tomlinson, J. M., Collins, D. R., Cubison, M. J., Dunlea, E. J., Huffman, J. A.,
922 Onasch, T. B., Alfarra, M. R., Williams, P. I., Bower, K., Kondo, Y., Schneider, J., Drewnick, F.,
923 Borrmann, S., Weimer, S., Demerjian, K., Salcedo, D., Cottrell, L., Griffin, R., Takami, A.,
924 Miyoshi, T., Hatakeyama, S., Shimono, A., Sun, J. Y., Zhang, Y. M., Dzepina, K., Kimmel, J. R.,
925 Sueper, D., Jayne, J. T., Herndon, S. C., Trimborn, A. M., Williams, L. R., Wood, E. C.,
926 Middlebrook, A. M., Kolb, C. E., Baltensperger, U. and Worsnop, D. R.: Evolution of organic
927 aerosols in the atmosphere, Science, 326(5959), 1525–1529, 2009.

928 Kamp, J. N., Chowdhury, A., Adamsen, A. P. S. and Feilberg, A.: Negligible influence of
929 livestock contaminants and sampling system on ammonia measurements with cavity ring-down
930 spectroscopy, Atmos. Meas. Tech., 12(5), 2837–2850, 2019.

931 Kim, H., Zhang, Q. and Heo, J.: Influence of intense secondary aerosol formation and long-range
932 transport on aerosol chemistry and properties in the Seoul Metropolitan Area during spring time:
933 results from KORUS-AQ, Atmos. Chem. Phys., 18(10), 7149–7168, 2018.

934 Kim, P. S., Jacob, D. J., Fisher, J. A., Travis, K., Yu, K., Zhu, L., Yantosca, R. M., Sulprizio, M.
935 P., Jimenez, J. L., Campuzano-Jost, P., Froyd, K. D., Liao, J., Hair, J. W., Fenn, M. A., Butler, C.
936 F., Wagner, N. L., Gordon, T. D., Welti, A., Wennberg, P. O., Crounse, J. D., St Clair, J. M.,
937 Teng, A. P., Millet, D. B., Schwarz, J. P., Markovic, M. Z. and Perring, A. E.: Sources,
938 seasonality, and trends of southeast US aerosol: an integrated analysis of surface, aircraft, and
939 satellite observations with the GEOS-Chem chemical transport model, Atmos. Chem. Phys., 15,
940 10411–10433, 2015.

941 Kline, J., Huebert, B., Howell, S., Blomquist, B., Zhuang, J., Bertram, T. and Carrillo, J.: Aerosol
942 composition and size versus altitude measured from the C-130 during ACE-Asia, J. Geophys.
943 Res., 109(D19), 340, 2004.

944 Klockow, D., Jablonski, B. and Nießner, R.: Possible artifacts in filter sampling of atmospheric
945 sulphuric acid and acidic sulphates, Atmos. Environ., 13(12), 1665–1676, 1979.

946 Koutrakis, P., Wolfson, J. M. and Spengler, J. D.: An improved method for measuring aerosol
947 strong acidity: Results from a nine-month study in St Louis, Missouri and Kingston, Tennessee,
948 Atmos. Environ., 22(1), 157–162, 1988.

949 Kupc, A., Williamson, C., Wagner, N. L., Richardson, M. and Brock, C. A.: Modification,
950 calibration, and performance of the Ultra-High Sensitivity Aerosol Spectrometer for particle size
951 distribution and volatility measurements during the Atmospheric Tomography Mission (ATom)
952 airborne campaign, Atmos. Meas. Tech., 11(1), 369–383, 2018.

953 Larson, T. V., Covert, D. S., Frank, R. and Charlson, R. J.: Ammonia in the human airways:
954 neutralization of inspired acid sulfate aerosols, Science, 197(4299), 161–163, 1977.

955 Lavery, T. F., Rogers, C. M., Baumgardner, R. and Mishoe, K. P.: Intercomparison of Clean Air

Status and Trends Network Nitrate and Nitric Acid Measurements with Data from Other Monitoring Programs, J. Air Waste Manag. Assoc., 59(2), 214–226, 2009.

Liao, J., Froyd, K. D., Murphy, D. M., Keutsch, F. N., Yu, G., Wennberg, P. O., St Clair, J. M., Crounse, J. D., Wisthaler, A., Mikoviny, T., Jimenez, J. L., Campuzano-Jost, P., Day, D. A., Hu, W., Ryerson, T. B., Pollack, I. B., Peischl, J., Anderson, B. E., Ziemba, L. D., Blake, D. R., Meinardi, S. and Diskin, G.: Airborne measurements of organosulfates over the continental U.S, J. Geophys. Res. D: Atmos., 120(7), 2990–3005, 2015.

Liggio, J., Li, S.-M., Vlasenko, A., Stroud, C. and Makar, P.: Depression of ammonia uptake to sulfuric acid aerosols by competing uptake of ambient organic gases, Environ. Sci. Technol., 45(7), 2790–2796, 2011.

Li, M., Weschler, C. J., Bekö, G., Wargocki, P., Lucic, G. and Williams, J.: Human Ammonia Emission Rates under Various Indoor Environmental Conditions, Environ. Sci. Technol., doi:10.1021/acs.est.0c00094, 2020.

Liu, C.-N., Lin, S.-F., Awasthi, A., Tsai, C.-J., Wu, Y.-C. and Chen, C.-F.: Sampling and conditioning artifacts of PM2.5 in filter-based samplers, Atmos. Environ., 85, 48–53, 2014.

Liu, C.-N., Lin, S.-F., Tsai, C.-J., Wu, Y.-C. and Chen, C.-F.: Theoretical model for the evaporation loss of PM2.5 during filter sampling, Atmos. Environ., 109, 79–86, 2015.

Liu, M., Huang, X., Song, Y., Tang, J., Cao, J., Zhang, X., Zhang, Q., Wang, S., Xu, T., Kang, L., Cai, X., Zhang, H., Yang, F., Wang, H., Yu, J. Z., Lau, A. K. H., He, L., Huang, X., Duan, L., Ding, A., Xue, L., Gao, J., Liu, B. and Zhu, T.: Ammonia emission control in China would mitigate haze pollution and nitrogen deposition, but worsen acid rain, Proc. Natl. Acad. Sci. U. S. A., 116(16), 7760–7765, 2019.

Liu, T., Clegg, S. L. and Abbatt, J. P. D.: Fast oxidation of sulfur dioxide by hydrogen peroxide in deliquesced aerosol particles, Proc. Natl. Acad. Sci. U. S. A., 117(3), 1354–1359, 2020.

Liu, X., Zhang, Y., Huey, L. G., Yokelson, R. J., Wang, Y., Jimenez, J. L., Campuzano-Jost, P., Beyersdorf, A. J., Blake, D. R., Choi, Y., St. Clair, J. M., Crounse, J. D., Day, D. A., Diskin, G. S., Fried, A., Hall, S. R., Hanisco, T. F., King, L. E., Meinardi, S., Mikoviny, T., Palm, B. B., Peischl, J., Perring, A. E., Pollack, I. B., Ryerson, T. B., Sachse, G., Schwarz, J. P., Simpson, I. J., Tanner, D. J., Thornhill, K. L., Ullmann, K., Weber, R. J., Wennberg, P. O., Wisthaler, A., Wolfe, G. M. and Ziemba, L. D.: Agricultural fires in the southeastern U.S. during SEAC[4]RS: Emissions of trace gases and particles and evolution of ozone, reactive nitrogen, and organic aerosol, J. Geophys. Res. D: Atmos., 121(12), 7383–7414, 2016.

Liu, X., Huey, L. G., Yokelson, R. J., Selimovic, V., Simpson, I. J., Müller, M., Jimenez, J. L., Campuzano-Jost, P., Beyersdorf, A. J., Blake, D. R., Butterfield, Z., Choi, Y., Crounse, J. D., Day, D. A., Diskin, G. S., Dubey, M. K., Fortner, E., Hanisco, T. F., Hu, W., King, L. E., Kleinman, L., Meinardi, S., Mikoviny, T., Onasch, T. B., Palm, B. B., Peischl, J., Pollack, I. B., Ryerson, T. B., Sachse, G. W., Sedlacek, A. J., Shilling, J. E., Springston, S., St. Clair, J. M.,

993 Tanner, D. J., Teng, A. P., Wennberg, P. O., Wisthaler, A. and Wolfe, G. M.: Airborne
994 measurements of western U.S. wildfire emissions: Comparison with prescribed burning and air
995 quality implications, J. Geophys. Res. D: Atmos., 122(11), 6108–6129, 2017.

996 Malm, W. C., Sisler, J. F., Huffman, D., Eldred, R. A. and Cahill, T. A.: Spatial and seasonal
997 trends in particle concentration and optical extinction in the United States, J. Geophys. Res.,
998 99(D1), 1347, 1994.

999 Malm, W. C., Schichtel, B. A., Hand, J. L. and Collett, J. L., Jr.: Concurrent Temporal and
1000 Spatial Trends in Sulfate and Organic Mass Concentrations Measured in the IMPROVE
1001 Monitoring Program, J. Geophys. Res. D: Atmos., 122(19), 10,462–10,476, 2017.

1002 Martin, N. A., Ferracci, V., Cassidy, N. and Hoffnagle, J. A.: The application of a cavity
1003 ring-down spectrometer to measurements of ambient ammonia using traceable primary standard
1004 gas mixtures, Appl. Phys. B, 122(8), 219, 2016.

1005 Ma, S.-S., Yang, W., Zheng, C.-M., Pang, S.-F. and Zhang, Y.-H.: Subsecond measurements on
1006 aerosols: From hygroscopic growth factors to efflorescence kinetics, Atmos. Environ., 210,
1007 177–185, 2019.

1008 McNaughton, C. S., Clarke, A. D., Howell, S. G., Pinkerton, M., Anderson, B., Thornhill, L.,
1009 Hudgins, C., Winstead, E., Dibb, J. E., Scheuer, E. and Maring, H.: Results from the DC-8 Inlet
1010 Characterization Experiment (DICE): Airborne versus surface sampling of mineral dust and sea
1011 salt aerosols, Aerosol Sci. Technol., 41(2), 136–159, 2007.

1012 Meskhidze, N., Chameides, W. L., Nenes, A. and Chen, G.: Iron mobilization in mineral dust:
1013 Can anthropogenic SO_2 emissions affect ocean productivity?, Geophys. Res. Lett., 30(21), 2085,
1014 2003.

1015 Mezuman, K., Bauer, S. E. and Tsigaridis, K.: Evaluating secondary inorganic aerosols in three
1016 dimensions, Atmos. Chem. Phys., 16(16), 10651–10669, 2016.

1017 Middlebrook, A. M., Bahreini, R., Jimenez, J. L. and Canagaratna, M. R.: Evaluation of
1018 Composition-Dependent Collection Efficiencies for the Aerodyne Aerosol Mass Spectrometer
1019 using Field Data, Aerosol Sci. Technol., 46(3), 258–271, 2012.

1020 Murphy, D. M. and Thomson, D. S.: Laser Ionization Mass Spectroscopy of Single Aerosol
1021 Particles, Aerosol Sci. Technol., 22(3), 237–249, 1995.

1022 Murphy, D. M., Froyd, K. D., Schwarz, J. P. and Wilson, J. C.: Observations of the chemical
1023 composition of stratospheric aerosol particles: The Composition of Stratospheric Particles, Q.J.R.
1024 Meteorol. Soc., 140(681), 1269–1278, 2014.

1025 Murray, B. J. and Bertram, A. K.: Inhibition of solute crystallisation in aqueous
1026 H+–NH4+–SO42−–H2O droplets, Phys. Chem. Chem. Phys., 10(22), 3287, 2008.

1027 Myhre, G., Shindell, D., Bréon, F.-M., Collins, W., Fuglestvedt, J., Huang, J., Koch, D.,

Atmospheric
Measurement
Techniques
Discussions

Open Access

EGU

Lamarque, J.-F., Lee, D., Mendoza, B., Nakajima, T., Robock, A., Stephens, G., Takemura, T. and Zhang, H.: Anthropogenic and Natural Radiative Forcing, in Climate Change 2013: The Physical Science Basis. Contribution of Working Group I to the Fifth Assessment Report of the Intergovernmental Panel on Climate Change, edited by T. F. Stocker, D. Qin, G.-K. Plattner, M. Tignor, S. K. Allen, J. Boschung, A. Nauels, Y. Xia, V. Bex, and P. M. Midgley, p. 659, Cambridge University Press, Cambridge, United Kingdom and New York, NY, USA., 2013.

National Research Council: The Airliner Cabin Environment and the Health of Passengers and Crew, The National Academies Press, Washington, DC., 2002.

Nault, B. A., Campuzano-Jost, P., Day, D. A., Schroder, J. C., Anderson, B., Beyersdorf, A. J., Blake, D. R., Brune, W. H., Choi, Y., Corr, C. A., de Gouw, J. A., Dibb, J., DiGangi, J. P., Diskin, G. S., Fried, A., Huey, L. G., Kim, M. J., Knote, C. J., Lamb, K. D., Lee, T., Park, T., Pusede, S. E., Scheuer, E., Thornhill, K. L., Woo, J.-H. and Jimenez, J. L.: Secondary Organic Aerosol Production from Local Emissions Dominates the Organic Aerosol Budget over Seoul, South Korea, during KORUS-AQ, Atmos. Chem. Phys., 18, 17769–17800, 2018.

Nenes, A., Pandis, S. N., Kanakidou, M., Russell, A., Song, S., Vasilakos, P. and Weber, R. J.: Aerosol acidity and liquid water content regulate the dry deposition of inorganic reactive nitrogen, Atmos. Phys. Chem. Discuss., doi:10.5194/acp-2020-266, 2020a.

Nenes, A., Pandis, S. N., Weber, R. J. and Russell, A.: Aerosol pH and liquid water content determine when particulate matter is sensitive to ammonia and nitrate availability, Atmos. Chem. Phys., 20(5), 3249–3258, 2020b.

Nguyen, T. K. V., Zhang, Q., Jimenez, J. L., Pike, M. and Carlton, A. G.: Liquid water: Ubiquitous contributor to aerosol mass, Environ. Sci. Technol. Lett., 3, 257–263, 2016.

Nie, W., Wang, T., Gao, X., Pathak, R. K., Wang, X., Gao, R., Zhang, Q., Yang, L. and Wang, W.: Comparison among filter-based, impactor-based and continuous techniques for measuring atmospheric fine sulfate and nitrate, Atmos. Environ., 44(35), 4396–4403, 2010.

Pagonis, D., Price, D. J., Algrim, L. B., Day, D. A., Handschy, A. V., Stark, H., Miller, S. L., de Gouw, J., Jimenez, J. L. and Ziemann, P. J.: Time-Resolved Measurements of Indoor Chemical Emissions, Deposition, and Reactions in a University Art Museum, Environ. Sci. Technol., 53(9), 4794–4802, 2019.

Paulot, F., Jacob, D. J., Johnson, M. T., Bell, T. G., Baker, A. R., Keene, W. C., Lima, I. D., Doney, S. C. and Stock, C. A.: Global oceanic emission of ammonia: Constraints from seawater and atmospheric observations, Global Biogeochem. Cycles, 29(8), 1165–1178, 2015.

Pratt, K. A. and Prather, K. A.: Aircraft measurements of vertical profiles of aerosol mixing states, J. Geophys. Res., 115(D11), D11305, 2010.

Price, H. C., Mattsson, J., Zhang, Y., Bertram, A. K., Davies, J. F., Grayson, J. W., Martin, S. T., O'Sullivan, D., Reid, J. P., Rickards, A. M. J. and Murray, B. J.: Water diffusion in atmospherically relevant α-pinene secondary organic material, Chem. Sci., 6(8), 4876–4883,

Atmospheric
Measurement
Techniques

Open Access

EGU

Discussions

1065 2015.

1066 Pye, H. O. T., Nenes, A., Alexander, B., Ault, A. P., Barth, M. C., Clegg, S. L., Collett, J. L., Jr.,
1067 Fahey, K. M., Hennigan, C. J., Herrmann, H., Kanakidou, M., Kelly, J. T., Ku, I.-T., McNeill, V.
1068 F., Riemer, N., Schaefer, T., Shi, G., Tilgner, A., Walker, J. T., Wang, T., Weber, R., Xing, J.,
1069 Zaveri, R. A. and Zuend, A.: The Acidity of Atmospheric Particles and Clouds, Atmos. Chem.
1070 Phys., 20(8), 4809–4888, 2020.

1071 Robbins, R. C. and Cadle, R. D.: Kinetics of the Reaction between Gaseous Ammonia and
1072 Sulfuric Acid Droplets in an Aerosol, J. Phys. Chem., 62(4), 469–471, 1958.

1073 Rumble, J. R., Ed.: CRC Handbook of Chemistry and Physics, 100th Edition, 2019 - 2020,
1074 Taylor & Francis Group., 2019.

1075 Schauer, C., Niessner, R. and Pöschl, U.: Polycyclic aromatic hydrocarbons in urban air
1076 particulate matter: decadal and seasonal trends, chemical degradation, and sampling artifacts,
1077 Environ. Sci. Technol., 37(13), 2861–2868, 2003.

1078 Schroder, J. C., Campuzano-Jost, P., Day, D. A., Shah, V., Larson, K., Sommers, J. M., Sullivan,
1079 A. P., Campos, T., Reeves, J. M., Hills, A., Hornbrook, R. S., Blake, N. J., Scheuer, E., Guo, H.,
1080 Fibiger, D. L., McDuffie, E. E., Hayes, P. L., Weber, R. J., Dibb, J. E., Apel, E. C., Jaeglé, L.,
1081 Brown, S. S., Thronton, J. A. and Jimenez, J. L.: Sources and Secondary Production of Organic
1082 Aerosols in the Northeastern US during WINTER, J. Geophys. Res. D: Atmos.,
1083 doi:10.1029/2018JD028475, 2018.

1084 Seinfeld., J. H. and Pandis, S. N.: Atmospheric Chemistry and Physics: From Air Pollution to
1085 Climate Change, Second., John Wiley & Sons, Inc., Hoboken, NJ USA., 2006.

1086 Shiraiwa, M., Ammann, M., Koop, T. and Pöschl, U.: Gas uptake and chemical aging of
1087 semisolid organic aerosol particles, Proc. Natl. Acad. Sci. U. S. A., 108(27), 11003–11008, 2011.

1088 Slade, J. H., Ault, A. P., Bui, A. T., Ditto, J. C., Lei, Z., Bondy, A. L., Olson, N. E., Cook, R. D.,
1089 Desrochers, S. J., Harvey, R. M., Erickson, M. H., Wallace, H. W., Alvarez, S. L., Flynn, J. H.,
1090 Boor, B. E., Petrucci, G. A., Gentner, D. R., Griffin, R. J. and Shepson, P. B.: Bouncier Particles
1091 at Night: Biogenic Secondary Organic Aerosol Chemistry and Sulfate Drive Diel Variations in
1092 the Aerosol Phase in a Mixed Forest, Environ. Sci. Technol., 53(9), 4977–4987, 2019.

1093 Solomon, P. A., Mitchell, W., Tolocka, M., Norris, G., Gemmill, D., Wiener, R., Vanderpool, R.,
1094 Murdoch, R., Natarajan, S. and Hardison, E.: Evaluation of PM2.5 Chemical Speciation
1095 Samplers for Use in the EPA National PM2.5 Chemical Speciation Network, EPA., 2000.

1096 Solomon, P. A., Crumpler, D., Flanagan, J. B., Jayanty, R. K. M., Rickman, E. E. and McDade,
1097 C. E.: U.S. national PM2.5 Chemical Speciation Monitoring Networks-CSN and IMPROVE:
1098 description of networks, J. Air Waste Manag. Assoc., 64(12), 1410–1438, 2014.

1099 Song, S., Gao, M., Xu, W., Shao, J., Shi, G., Wang, S., Wang, Y., Sun, Y. and McElroy, M. B.:
1100 Fine-particle pH for Beijing winter haze as inferred from different thermodynamic equilibrium

models, Atmos. Chem. Phys., 18(10), 7423–7438, 2018.

Spiller, L. L.: Determination of Ammonia/Air Diffusion Coefficient Using Nafion Lined Tube, Anal. Lett., 22(11-12), 2561–2573, 1989.

Stith, J. L., Ramanathan, V., Cooper, W. A., Roberts, G. C., DeMott, P. J., Carmichael, G., Hatch, C. D., Adhikary, B., Twohy, C. H., Rogers, D. C., Baumgardner, D., Prenni, A. J., Campos, T., Gao, R., Anderson, J. and Feng, Y.: An overview of aircraft observations from the Pacific Dust Experiment campaign, J. Geophys. Res., 114(D5), 833, 2009.

Sueper, D.: ToF-AMS Data Analysis Software Webpage, [online] Available from: http://cires1.colorado.edu/jimenez-group/wiki/index.php/ToF-AMS_Analysis_Software, 2018.

Sun, K., Cady-Pereira, K., Miller, D. J., Tao, L., Zondlo, M. A., Nowak, J. B., Neuman, J. A., Mikoviny, T., Müller, M., Wisthaler, A., Scarino, A. J. and Hostetler, C. A.: Validation of TES ammonia observations at the single pixel scale in the San Joaquin Valley during DISCOVER-AQ, J. Geophys. Res. D: Atmos., 120(10), 5140–5154, 2015.

Sun, Y., Zhang, Q., Macdonald, A. M., Hayden, K., Li, S. M., Liggio, J., Liu, P. S. K., Anlauf, K. G., Leaitch, W. R., Steffen, A., Cubison, M., Worsnop, D. R., van Donkelaar, A. and Martin, R. V.: Size-resolved aerosol chemistry on Whistler Mountain, Canada with a high-resolution aerosol mass spectrometer during INTEX-B, Atmos. Chem. Phys., 9(9), 3095–3111, 2009.

Sutton, M. A., Dragosits, U., Tang, Y. S. and Fowler, D.: Ammonia emissions from non-agricultural sources in the UK, Atmos. Environ., 34(6), 855–869, 2000.

Swartz, E., Shi, Q., Davidovits, P., Jayne, J. T., Worsnop, D. R. and Kolb, C. E.: Uptake of Gas-Phase Ammonia. 2. Uptake by Sulfuric Acid Surfaces, J. Phys. Chem. A, 103(44), 8824–8833, 1999.

Talbot, R. W., Dibb, J. E., Lefer, B. L., Scheuer, E. M., Bradshaw, J. D., Sandholm, S. T., Smyth, S., Blake, D. R., Blake, N. J., Sachse, G. W., Collins, J. E. and Gregory, G. L.: Large-scale distributions of tropospheric nitric, formic, and acetic acids over the western Pacific basin during wintertime, J. Geophys. Res.: Atmos., 102(D23), 28303–28313, 1997.

Tao, Y. and Murphy, J. G.: The sensitivity of $PM_{2.5}$ acidity to meteorological parameters and chemical composition changes: 10-year records from six Canadian monitoring sites, Atmos. Chem. Phys., 19(14), 9309–9320, 2019.

Thomson, D. S., Schein, M. E. and Murphy, D. M.: Particle Analysis by Laser Mass Spectrometry WB-57F Instrument Overview, Aerosol Sci. Technol., 33(1-2), 153–169, 2000.

Toon, O. B., Maring, H., Dibb, J., Ferrare, R., Jacob, D. J., Jensen, E. J., Luo, Z. J., Mace, G. G., Pan, L. L., Pfister, L., Rosenlof, K. H., Redemann, J., Reid, J. S., Singh, H. B., Thompson, A. M., Yokelson, R., Minnis, P., Chen, G., Jucks, K. W. and Pszenny, A.: Planning, implementation, and scientific goals of the Studies of Emissions and Atmospheric Composition, Clouds and Climate Coupling by Regional Surveys (SEAC[4]RS) field mission, J. Geophys. Res. D: Atmos.,

121(9), 4967–5009, 2016.

Vay, S. A., Woo, J.-H., Anderson, B. E., Thornhill, K. L., Blake, D. R., Westberg, D. J., Kiley, C. M., Avery, M. A., Sachse, G. W., Streets, D. G., Tsutsumi, Y. and Nolf, S. R.: Influence of regional-scale anthropogenic emissions on CO_2 distributions over the western North Pacific, J. Geophys. Res., 108(D20), 213, 2003.

Vay, S. A., Choi, Y., Vadrevu, K. P., Blake, D. R., Tyler, S. C., Wisthaler, A., Hecobian, A., Kondo, Y., Diskin, G. S., Sachse, G. W., Woo, J.-H., Weinheimer, A. J., Burkhart, J. F., Stohl, A. and Wennberg, P. O.: Patterns of CO_2 and radiocarbon across high northern latitudes during International Polar Year 2008, J. Geophys. Res., 116(D14), 4039, 2011.

Walker, J. M., Philip, S., Martin, R. V. and Seinfeld, J. H.: Simulation of nitrate, sulfate, and ammonium aerosols over the United States, Atmos. Chem. Phys., 12(22), 11213–11227, 2012.

Wang, J., Hoffmann, A. A., Park, R. J., Jacob, D. J. and Martin, S. T.: Global distribution of solid and aqueous sulfate aerosols: Effect of the hysteresis of particle phase transitions, J. Geophys. Res., 113(D11), 1770, 2008a.

Wang, J., Jacob, D. J. and Martin, S. T.: Sensitivity of sulfate direct climate forcing to the hysteresis of particle phase transitions, J. Geophys. Res., 113(D11), 13791, 2008b.

Warneke, C., Schwarz, J. P., Ryerson, T., Crawford, J., Dibb, J., Lefer, B., Roberts, J., Trainer, M., Murphy, D., Brown, S., Brewer, A., Gao, R.-S. and Fahey, D.: Fire Influence on Regional to Global Environments and Air Quality (FIREX-AQ): A NOAA/NASA Interagency Intensive Study of North American Fires, NOAA/NASA. [online] Available from: https://esrl.noaa.gov/csd/projects/firex-aq/whitepaper.pdf, 2018.

Warner, J. X., Wei, Z., Larrabee Strow, L., Dickerson, R. R. and Nowak, J. B.: The global tropospheric ammonia distribution as seen in the 13-year AIRS measurement record, Atmos. Chem. Phys., 16(8), 5467–5479, 2016.

Warner, J. X., Dickerson, R. R., Wei, Z., Strow, L. L., Wang, Y. and Liang, Q.: Increased atmospheric ammonia over the world's major agricultural areas detected from space, Geophys. Res. Lett., 44(6), 2875–2884, 2017.

Watson, J. G., Chow, J. C., Chen, L. W. A. and Frank, N. H.: Methods to assess carbonaceous aerosol sampling artifacts for IMPROVE and other long-term networks, J. Air Waste Manag. Assoc., 59(8), 898–911, 2009.

Weber, R. J., Orsini, D., Daun, Y., Lee, Y.-N., Klotz, P. J. and Brechtel, F.: A Particle-into-Liquid Collector for Rapid Measurement of Aerosol Bulk Chemical Composition, Aerosol Sci. Technol., 35(3), 718–727, 2001.

Weber, R. J., Guo, H., Russell, A. G. and Nenes, A.: High aerosol acidity despite declining atmospheric sulfate concentrations over the past 15 years, Nat. Geosci., 9(4), 282–285, 2016.

1172 Williamson, C., Kupc, A., Wilson, J., Gesler, D. W., Reeves, J. M., Erdesz, F., McLaughlin, R.
1173 and Brock, C. A.: Fast time response measurements of particle size distributions in the 3–60 nm
1174 size range with the nucleation mode aerosol size spectrometer, Atmos. Meas. Tech., 11(6),
1175 3491–3509, 2018.

1176 Wilson, R. E.: Humidity Control by Means of Sulfuric Acid Solutions, with Critical Compilation
1177 of Vapor Pressure Data, J. Ind. Eng. Chem., 13(4), 326–331, 1921.

1178 Worsnop, D. R., Williams, L. R., Kolb, C. E., Mozurkewich, M., Gershenzon, M. and
1179 Davidovits, P.: Comment on "The NH_3 Mass Accommodation Coefficient for Uptake onto
1180 Sulfuric Acid Solution," J. Phys. Chem. A, 108(40), 8546–8548, 2004.

1181 Yao, X. H. and Zhang, L.: Supermicron modes of ammonium ions related to fog in rural
1182 atmosphere, Atmos. Chem. Phys., 12(22), 11165–11178, 2012.

1183 Zakoura, M., Kakavas, S., Nenes, A. and Pandis, S. N.: Size-resolved aerosol pH over Europe
1184 during summer, Atmos. Chem. Phys. Discuss., doi:10.5194/acp-2019-1146, 2020.

1185 Zhang, X., Smith, K. A., Worsnop, D. R., Jimenez, J., Jayne, J. T. and Kolb, C. E.: A Numerical
1186 Characterization of Particle Beam Collimation by an Aerodynamic Lens-Nozzle System: Part I.
1187 An Individual Lens or Nozzle, Aerosol Sci. Technol., 36(5), 617–631, 2002.

1188 Zhang, X., Smith, K. A., Worsnop, D. R., Jimenez, J. L., Jayne, J. T., Kolb, C. E., Morris, J. and
1189 Davidovits, P.: Numerical Characterization of Particle Beam Collimation: Part II Integrated
1190 Aerodynamic-Lens–Nozzle System, Aerosol Sci. Technol., 38(6), 619–638, 2004.

1191 Zhou, S., Collier, S., Jaffe, D. A. and Zhang, Q.: Free tropospheric aerosols at the Mt. Bachelor
1192 Observatory: more oxidized and higher sulfate content compared to boundary layer aerosols,
1193 Atmos. Chem. Phys., 19(3), 1571–1585, 2019.

1194